AUT Journal of Mechanical Engineering

AUT J. Mech. Eng., 4(3) (2020) 363-380
DOI: 10.22060/ajme.2019.16362.5816

Effect of Spinning Speed Fluctuation along with the Twist Angle on the Nonlinear Vibration and Stability of an Asymmetrical Twisted Slender Beam

M. Tajik, A. Karami Mohammadi*

Faculty of Mechanical Engineering, Shahrood University of Technology, Shahrood, Iran

ABSTRACT: In this study, the effect of spinning speed fluctuations along with the twist angle, on the stability and bifurcation of spinning slender twisted beams, with linear twist angle and large transverse deflections, near the primary and parametric resonances have been analyzed using the Euler–Bernoulli model. The spinning speed fluctuation along with the twist angle, asymmetry and imbalance, play an important role on the frequency response of the twisted beam. The equations of motion, in the case of pure single mode motion, are analyzed by using the multiple scales method after discretization by the Galerkin's procedure. The instability of the twisted and untwisted beams is investigated and cases and domains are determined in which bifurcation could occur. Effects of the speed fluctuations, twist angle, damping ratio, asymmetry, eccentricity and mass moment of inertia about the longitudinal axis on the frequency response of the twisted beam are investigated. This is explained that the spinning speed fluctuation effect is weak in lower modes and smaller twist angles while asymmetry effect is dominant. By ascending the mode number and twist angle, spinning speed fluctuation effect amplifies the amplitude of system. The results are compared and validated with the results obtained from Runge-Kutta numerical method in steady state, and confirmed with some previous researches.

Review History:

Received: 2019-05-20
Revised: 2019-07-12
Accepted: 2019-09-22
Available Online: 2019-10-04

Keywords:

Spinning speed fluctuations
Bifurcation analysis
Twist angle
Multiple scales method
Galerkin's method

1. INTRODUCTION

The analysis of the behavior of rotating systems plays an important role in reducing the destructive vibrations of rotating systems such as turbine blades, helicopter rotor blades, pumps, compressors, satellite booms and machining (fluted end-milling cutter, drilling, and boring bar). In reality, these systems may be subjected to torsional loads and thus spinning fluctuates. These perturbations can produce devastating effects on such equipment. Therefore, studying the nonlinear vibrational and dynamic behavior of twisted and non-twisted beams is of great importance and can help to understand the behavior of more complex structures under similar conditions. In recent years, numerous studies have been conducted on the vibrational behavior of twisted beams. These beams are usually introduced using Euler-Bernoulli and Timoshenko models and their twist angles may be linear or non-linear along the longitudinal axis of the beam. Some of the analyses focus on the non-rotating twisted beams and rotating twisted beams about the perpendicular direction. Early success in modeling of the twisted beams obtained by Washizu [1]. He explained that the twisted beams have made of flat fibers which have been twisted spirally and make a twisted beam. Also, he extracted mathematical equations of the twisted cantilever beam and used semi-inverse technique to analyze the dynamical behavior of the twisted beam by considering the torsional and flexural deformations. Slyper [2] studied the coupled bending-bending vibrations of a twisted cantilevered beam. By extracting the resonance frequencies and the equations of motion, frequencies and modal curves of experimental and theoretical models obtained for three twist angles 0° and 90°, and indicated a good correlation together. Carnegie [3] presented transverse vibration equations by considering the coupling between bending and rotation and investigated the geometrical effects of twisted beams on natural frequencies. Dawson and Carnegie [3] predicted modal curves despite the stress along the turbine blades. The prediction results depend on the torsion angle, cross-section, centrifugal tension and aerodynamic effects. Turbine blades are modeled as rectangular twisted beams with varying length-to-width ratios and torsion angles of 0 to 90 degrees. The results are compared with similar work and show good agreement. Imregun [4] used a numerical method to investigate the frequency response of turbomachinery blades. He modelled the blades as rotary twisted beam and extracted the equations of motion by considering the Coriolis effects, and found that the obtained results have a good correlation with the previous researches. Oh et al. [5] studied coupled vibrations of the rotating twisted composite beams by considering the shear effects and inertia terms. They extracted the equations by using the Hamilton's principle and investigated influences of the number of layers and

*Corresponding author's email: akaramim@yahoo.com

twist angle on the frequency response curves. Banerjee [6] used a dynamic stiffness method to determine the natural frequency of a non-rotating twisted beam. Rotational inertia and shear deformation of the twisted beam were considered, and the success of this method for obtaining system eigenfrequencies was elucidated. Yardimoglu and Yildirim [7] have succeeded in introducing a new method based on the finite element method to obtain resonant frequencies of non-spinning pre-twisted Timoshenko beams. Sabuncu and Evran [8] investigated the effect of twist angle on the frequency responses of linear and nonlinear twisted blades about the transverse axis and found that the relationship between linear and nonlinear blade models was smaller for larger twist angles. Lin et al. [9] obtained the transverse vibration equations of a twisted beam mounted on an elastic foundation. They studied the frequency response of the beam in three states under damping, critical and overdamping, and the effect of parameters such as twist angle, and damping ratio on the frequency response and system instability. Avramov and Pierre [10] modeled the rotating blade as a rotating asymmetric twisted beam and obtained the nonlinear partial differential. They used the Galerkin method to discretize the equations. Also, they used the nonlinear normal mode method to analyze the set of equations and found that first and fourth backbone curves are soft and the second and third backbone curves are hard. Verichev et al. [11] studied vibration behavior of a rotary system with harmonic speed and without changing in the visco-elastic properties of the system. They applied averaging method and numerical integration to validate analytical results and shown that vibrations of the system could be damped by selecting the suitable parameters for the harmonic term of rotation speed. Yao et al. [12] investigated the nonlinear stability of the rotating blade with speed fluctuation under high-temperature supersonic gas flow. They modeled the rotating blade as a pre-twist, thin-walled rotating cantilever beam and used the isotropic constitutive law and Hamilton's principle to extract the nonlinear partial differential equations of motion. Aerodynamic loads were explained by first-order piston theory. Then, they discretized the obtained equations by Galerkin's method and applied the method of the multiple scales to describe the internal and primary resonances. Finally, they found that there are the periodic and chaotic motions in this system with speed fluctuation. Ebrahimi and Mokhtari [13] presented free vibration analysis of rotating exponentially graded thick beams based on the Timoshenko beam theory. They used Hamilton's principle to extract the equations and solved them by the differential transform method. They studied the influences of the constituent volume fractions, slenderness ratios, rotational speed and hub radius on the vibration characteristics of the rotating thick Functionally Graded (FG) beam and indicated that these effects play significant role on the dynamic behavior of rotating FG beam. Bekir et al. [14] studied dynamical behavior of spinning twisted beam by considering the Coriolis effects. They performed their analysis using the Spectral-Tchebychev method and compared the results with the finite element simulation results. The study showed that both results agree with good accuracy. They also found that the aforementioned three-dimensional approach can be applied to more complex structures and boundary conditions. Adair and Jaeger [15] investigated vibration of the rotating twisted Euler–Bernoulli beams using the modified adomian decomposition method. They obtained the linear differential equations of motion considering the centrifugal stiffness. Natural frequency and mode shapes obtained simultaneously using the Adomian Modified Decomposition Method (AMDM). AMDM converts the motion equations to recursive algebraic equations and simple algebraic boundary conditions.

However, work on twisted beam vibrations spinning around its longitudinal axis is scarce. Tekinalp and Ulsoy [16,17] described instability and vibrational response of a drill bit as the spinning twisted beam about its longitudinal axis and investigated influences of the twist angle, rotational speed and aspect ratio on the transverse frequency response. They modeled twisted beam as Euler-Bernoulli beam and utilized the finite element method and compared results with analytical and experimental procedures. Huang [18] simulated a drilling bit with the Winkler foundation and investigated the impact of structural damage on the stability of the twisted beam with time-dependent boundary conditions. He investigated the stability of the bit by changing drilling force. Young and Gau [19] investigated instability of spinning pre-twisted beams about the longitudinal axis with simple periodic speed and Gaussian white noise axial force as a summation of the static and dynamic forces using the finite element method. They found that there are unstable domains in main resonances and instability domains reduce at the higher resonances. Furthermore, results were extracted numerically for different combination resonances. Gurgeoze [20] studied axial force vibration of a pre-twisted rotor and solved linear equations of motion by Galerkin's method. He used the multiple scales procedure explained vibrational responses for several and the results boundary conditions. Lee [21,22] analyzed stability of twisted beam with simply support and clamp-free boundary conditions. He used Euler-Bernoulli beam theory and utilized assumed mode method to investigate the stability domains of the beam. Above mentioned beam is under constant and sinusoidal axial load. The obtained results indicated that the spinning speed, the twist angle and the slenderness coefficient of the beam effect on the stability regions. Tan et al. [23] obtained the equations of motion of the twisted beam with zero and non-zero twist angle. The beam was modelled by Euler beam theory and was under axial force. They utilized the assumed mode method and concluded that ascending the twist angle, unstable domain increases. Chen [24] presented the instability results of a rotating twisted beam about the axial direction and under the axial force. He modelled twisted beam with Timoshenko theory and considered Coriolis effect. The equations of motion obtained in coordinate system attached to the twisted beam by Hamilton's principle and were discretized by the finite element. He studied influences the twist angle, rotating speed, constant axial load and slenderness coefficient. Once again, Chen et al. [25] analyzed the vibration behavior of the spinning twisted beam by ANSYS software. Chen et al. [26] investigated the instability of a pre-twisted beam under a periodic axial load. The beam was viscoelastic and rotated about the axial direction of beam. They used Hamilton's principle to obtain the equations and discretized equations by finite element method. By considering Bolotin's method, influences of spinning speed, twist angle, setting angle and constant axial load were studied on the stability regions. Chen [27] studied vibrational behavior of twisted beam based on the Timoshenko theory and Kelvin-Voigt damping in varies boundary conditions. To simplifying, he used coordinate frame attached to fluted frame and obtained the equations of motion linearly by finite element method. He described that descending the internal damping increases imaginary part of the eigenfrequencies while twist angle decreases. In other research, Chen [28] studied the axial load effect on the vibrational responses twisted Timoshenko beams with Kelvin-Voigt damping. He presented the previous results in above mentioned cases. Li et al. [29] presented free vibration of a spinning composite thin-walled beam with hydrothermal conditions. They utilized Hamilton's principle to extract the equations of motion based on the constitutive relationship and solved the obtained equations by Galerkin's discretization method. They investigated influences of the moisture, spinning speed, temperature and fiber orientation angles on the frequency responses of the beam and found that ascending the spinning speed decreases natural frequency of the vertical beam while increases natural frequency of the horizontal beam. Also, the natural frequencies decrease and increase with respect to the length-to-radius ratio and thickness-to-radius ratio, respectively. Li et al. [30] studied the coupled vibrations of a spinning composite thin-walled beam with the axial moving. They extracted motion equations by Hamilton's principle and discretized them by Galerkin's method. The effects of the fiber orientation angles, length-and thickness-to-radius ratios, axially moving speeds and spinning speeds on the natural frequencies of the beam were studied and they found that the natural frequencies of vertical beam decrease with respect to the spinning angular speed, while it is unlike for the horizontal beam. But, the natural frequencies of vertical and horizontal beam decrease with respect to the axial speed. Zhu and Chung [31] investigated a new model of spinning beam with deployment based on the Rayleigh beam theory and obtained coupled equations of motion by using the von Karman nonlinear strain theory. Galerkin's method was applied to discretize the equations and natural frequencies of the Rayleigh and Euler–Bernoulli beams were compared by considering the deploying motions. They explained that Rayleigh beam model is more exact than the Euler–Bernoulli beam model, because the rotary inertia effect is accounted for the Rayleigh beam model. Also, flexural motion of the Rayleigh beam is influenced by both of the deployment and spinning speed, while flexural motion of the Euler–Bernoulli beam is influenced by only the deployment speed. Zhu and Chung [32] studied the stability of a simply supported spinning beam with an axially moving motion. They extracted natural frequencies of the beam and investigated the critical speed and stability domains. In this study, they found that the present equations of motion are more reliable than the previous equations because the present equations completely consider the rotary inertia terms. Thomas et al. [33] explained the nonlinear vibrations of the cantilever beam and studied the influence of the rotational speed on the hardening and softening behavior and the bifurcation points. Equations of motion were analyzed analytically and discretized by finite element method. They compared the maximum amplitude of vibrations with both of the above-mentioned methods and investigated the accuracy of the results together. Sheng and Wang [34] studied nonlinear dynamic behavior of the Euler–Bernoulli beams with the simply support boundary conditions, moving load and Kelvin–Voigt damping. They extracted the nonlinear partial differential equations of the motion by using the Von Karman nonlinear theory and D'Alembert's principle and discretized them by the Galerkin's method. The results shown that the amplitude of nonlinear system responses are higher than that obtained from the linear system. Farsadi et al. [35] studied aero-elastic response of the blades modeled by asymmetric composite pre-twisted rotating thin walled beams. They used Hamilton's principle to extract the equations of motion and boundary conditions and the approximation of Green-Lagrange strain tensor to extract the strain field of the system. The equations were discretized by Galerkin's method and findings were concentrated on the effects of the coupling in circumferentially asymmetric stiffness and circumferentially uniform stiffness configurations, twist angle, rotating speed and fiber orientation, on the natural frequencies of the beam. Mirtalaei and Hajabasi [36] studied axial, bending and torsional vibrations of the in-extensional rotating beam. Equations of motion were solved by perturbation method and investigated influences of the coupling axial, bending and torsional motion, rotating speed and radius to length ratio of the beam on the vibration behavior of system. Qaderi et al. [37] presented the nonlinear dynamic behavior of a spinning shaft with the parametric and external excitations. They explained that external excitation is due to shaft unbalance and parametric excitation is due to periodic axial force, and investigated combination resonances of parametric excitation and primary resonance of external force. In this work, the multiple scales method was applied to ordinary nonlinear differential equations and the influence of various parameters on the response of the system was studied. Xinwei and Zhang [38] used the quadrature element technique to solve the coupled dynamic behavior of curved and pre-twisted beam like structures with irregular shapes of cross-section. Beams were rectangular, circular, elliptical and airfoil cross-sections, various curvature and pre-twist rates, and different boundary conditions. They obtained the results and compared them with the 3Dimensioal Spectral-Tchebychev (3D-ST) solutions and the finite element data, and indicated that the proposed method is accurate when the number of degrees of freedom is small. Karimi Nobandegani et al. [39] presented instability of twisted beam with clamp-free boundary condition under axial load so that the beam rotates about the axial direction in a viscoelastic Kelvin-Voigt foundation. They extracted the equations of motion by Hamilton's principle discretized them by finite element method. Finally, stability of the system was studied by changing the force coefficient, damping ratio, twist angle and slenderness coefficient. Tajik and Karami Mohammadi [40] investigated the nonlinear bifurcation and stability of the Euler-Bernoulli twisted beam assuming it was slender, asymmetric and unbalanced. They studied influences of the twist angle, damping ratio and eccentricity on the frequency responses and found that the frequency response curves in the first two modes are of hardening type. So that increasing the torsion angle in the first mode can reduce the amplitude of the steady oscillation while in the second mode it reverses. As presented above, methods used to analyze the twisted beams are discretization methods such as finite element and Galerkin methods and the twisted beams often have been analyzed linearly, while practically the behavior of the twisted beams is nonlinear. Furthermore, in general, all studies are about the twisted beams without any eccentricities and fluctuations on the spinning speed, while in fact, twisted beams may be imbalance and asymmetrical with the spinning speed fluctuations. So, identifying and improving their vibrational behavior play an important role in the vibrational motion of the rotary systems. In reference [40], the twisted beam was symmetric and spins with constant speed.

In this paper, the twisted beam is asymmetric and its rotational speed fluctuates. The effects of speed fluctuations and twisted angles by considering the asymmetric and unbalance are studied on the vibrational behavior of the pre-twisted Euler-Bernoulli beams that spin about the longitudinal axis. Hence, excitation sources are the imbalance, asymmetry and speed fluctuation and influences of the gyroscopic and rotary inertia are considered. The obtained equations of motion are analyzed in the case of single mode motion by Galerkin's discretization method and then multiple scales method is applied on the obtained ordinary differential equations. The instability of the twisted and untwisted beams is investigated and cases and domains are determined that bifurcation can occur. Furthermore, the results are validated using the Runge-Kutta numerical method in the steady state.

2. GOVERNING EQUATIONS OF MOTION

Consider a slender asymmetrical twisted beam that spins about the axial direction with varying speed and simply-simply boundary condition in Fig. 1. The frames X-Y-Z and $\zeta-\eta-\xi$ are fixed and twisted coordinate systems, respectively. The twist angle changes in linear form by $\beta_0 x$ (β_0 is pre-twist angle per unit length) so that the local coordinate $\zeta-\eta-\xi$ twists on the flute of beam. ξ and η are principle axes of the beam cross-section, and X and ζ are coincident. The beam is isotropic and Euler-Bernoulli theory has been utilized so that the shape of the cross-section and all its geometrical dimensions remain invariant in its plane. Also, rotary inertia and gyroscopic effects have been considered. Three successive Euler-angles $\psi(t,x)$, $\theta(t,x)$ and $\phi(t,x)$ about the axes of X, Y, Z [41] are used to indicate the rotation of the cross-section of beam. $\psi(t,x)$ and $\theta(t,x)$ are due to the flexural deformation of the beam and $\phi(t,x)$ is only due to the spinning speed of the twisted beam. By assuming the torsional deformation is small, $\phi(t,x)$ is,

$$\phi(t,x)=\int_0^t \Omega(t)dt \tag{1}$$

Assume the spinning speed of the simply supported twisted beam is under a sinusoidal perturbation as following,

$$\Omega(t)=\Omega_0\left(1+\varepsilon^2\cos(2\Omega t)\right) \tag{2}$$

So, substituting Eq. (2) into Eq. (1) gives,

$$\phi(t,x)=\Omega_0\left(t+\frac{\varepsilon^2}{2\Omega}\sin(2\Omega t)\right) \tag{3}$$

From the Euler angles, angular velocity and curvature components of the spinning twisted beam in XYZ frame can be written the same as in reference [40]. Extracting the partial differential equations of motion is done by using Hamilton's principle as following,

$$\int_{t_1}^{t_2} \delta\mathcal{L}dt=0 \tag{4}$$

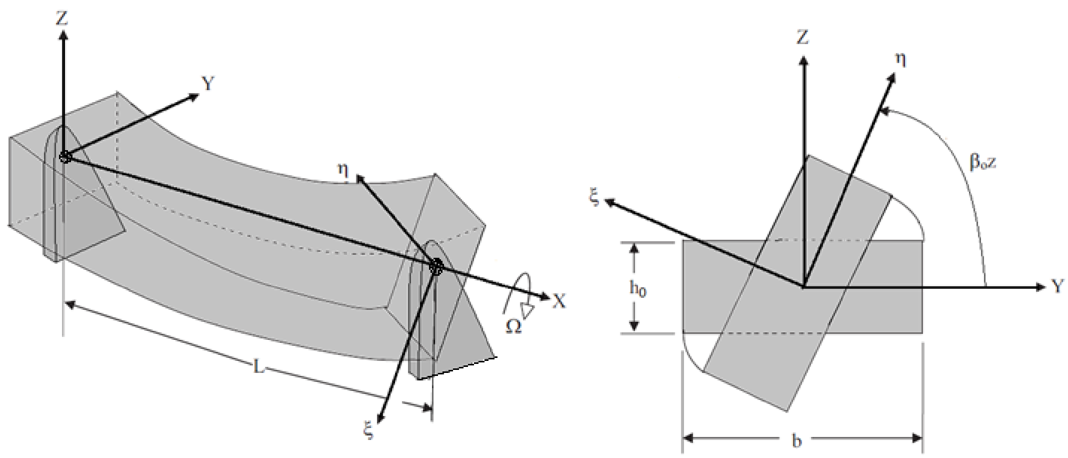

Fig. 1. Spinning pre-twisted beam with two coordinate frames fixed (XYZ) and local ($\zeta\eta\xi$).

where $\mathcal{L} = T - U + W_{nc}$. T, U, and W_{nc} denote to the kinetic, potential and external non-conservative energies. The kinetic and potential energies of the spinning twisted beam can be calculated the same as in reference [40]. By neglecting the internal damping and considering the external damping in transverse directions of Y and Z as $c_v = c_w = c$, So, dissipation energy, W_{nc} , is given the same as in reference [40]. From the Fig. 1, displacement components of the center of mass of the beam in the global coordinate XYZ are $u_x(t,x)$, $v_y(t,x)$ and $w_Z(t,x)$. By considering the displacement components of the natural axis of the twisted beam in the local coordinate $\zeta\eta\xi$ as $u_\zeta(t,x)$, $v_\eta(t,x)$ and $w_\xi(t,x)$, rotational matrix $\Re$ is used to describe the displacement components of these frames in a single equation and convert them together as following,

$$\Re = \begin{bmatrix} 1 & 0 & 0 \\ 0 & \cos(\beta_0 x) & -sin(\beta_0 x) \\ 0 & \sin(\beta_0 x) & \cos(\beta_0 x) \end{bmatrix} \tag{5}$$

Hence,

$$\begin{Bmatrix} u_x \\ v_y \\ w_z \end{Bmatrix} = \Re \begin{Bmatrix} u_\zeta \\ v_\eta \\ w_\xi \end{Bmatrix} \tag{6}$$

Similarly, moments of inertia and stiffness matrices between the XYZ and $\zeta\eta\xi$ frames can be expressed as,

$$\begin{bmatrix} I_{xx} & 0 & 0 \\ 0 & I_{yy} & I_{yz} \\ 0 & I_{zy} & I_{zz} \end{bmatrix} = \Re \begin{bmatrix} I_{\zeta\zeta} & 0 & 0 \\ 0 & I_{\eta\eta} & 0 \\ 0 & 0 & I_{\xi\xi} \end{bmatrix} \Re^T \tag{7}$$

and

$$\begin{bmatrix} D_{xx} & 0 & 0 \\ 0 & D_{yy} & D_{yz} \\ 0 & D_{zy} & D_{zz} \end{bmatrix} = \Re \begin{bmatrix} D_{\zeta\zeta} & 0 & 0 \\ 0 & D_{\eta\eta} & 0 \\ 0 & 0 & D_{\xi\xi} \end{bmatrix} \Re^T$$

Where

$$I_{\xi\xi} = \iint_A \rho\eta^2 d\eta d\xi \ , \ I_{\zeta\zeta} = \iint_A \rho(\eta^2 + \xi^2) d\eta d\xi \ ,$$

$$I_{\eta\eta} = \iint_A \rho\xi^2 d\eta d\xi \tag{8}$$

$$D_{\zeta\zeta} = G\iint_A (\eta^2 + \xi^2) d\eta d\xi \ , \ D_{\xi\xi} = E\iint_A \eta^2 d\eta d\xi \ ,$$

$$D_{\eta\eta} = E\iint_A \xi^2 d\eta d\xi \ , \ A_{xx} = A_{\zeta\zeta} = E\iint_A d\eta d\zeta \tag{9}$$

where $\Re^T$ is the transpose matrix of $\Re$ and, ρ , A, E and G are mass density, area cross-section, elasticity and shear modules of the twisted beam, respectively. Advantage of using the twisted frame $\zeta\eta\xi$ to extract the equations is that cross-sectional properties of the twisted beam such as principal moments of inertia do not vary along the longitudinal axis. The twisted beam has imbalance defined by (e_η, e_ξ) . So, displacement components of the center of mass can be written as,

$$u_{Gx} = u_x, \quad v_{Gy} = v_y + e_\eta \cos(\Omega t) - e_\xi \sin(\Omega t),$$

$$w_{Gz} = w_z + e_\eta \sin(\Omega t) + e_\xi \cos(\Omega t) \tag{10}$$

Longitudinal strain of centroidal line of the twisted beam e can be calculated as [40]

$$e = \sqrt{(1+u'_x)^2 + {v'_y}^2 + {w'_z}^2} - 1 \tag{11}$$

The rotational Euler angles ψ and θ can be obtained as following [40],

$$sin\psi = \frac{v'_y}{\sqrt{(1+u'_x)^2 + {v'_y}^2}} \ ,$$

$$sin\theta = \frac{-w'_z}{\sqrt{(1+u'_x)^2 + {v'_y}^2 + {w'_z}^2}} \tag{12}$$

Since the Euler angles of the ψ and θ are dependent variables, the number of independent variables is reduced to three translational displacements u_x , v_y and w_Z . Finally, by considering the Eqs. (1) to (12), expanding the angular velocities and curvatures by Taylor series up to $O(\varepsilon^3)$, converting the displacement, mass moments of inertia and stiffness components to twisted frame $\zeta\eta\xi$, substituting results in the kinetic, potential and dissipation energies and applying the Hamilton's principle, Eq. (4), the partial differential equations of motion of the spinning twisted beam with speed fluctuation in the twisted frame can be written as following,

$$m\ddot{u} - A_{xx}\Big(u'' + w'w'' + v'v'' + \beta_0(vw'' - wv'')$$

$$+ \beta_0^2(vv' + ww')\Big) = 0 \tag{13}$$

$$
\begin{aligned}
& m\ddot{Z}+\Sigma DZ^{(4)}-\Sigma I\ddot{Z}''-2i\beta_0^3\Sigma DZ'-\beta_0^2\left(-\Sigma I\ddot{Z}+5\Sigma DZ''\right)-i\beta_0\left(2\Sigma I\ddot{Z}'-4Z'''\right)+c\dot{Z}e^{i\beta_0x}+\Big[\left(1/2i\bar{Z}'Z^2+iZZ'\bar{Z}\right)\beta_0{}^3 \\
& +\left(-Z''Z\bar{Z}-Z'^2\bar{Z}+1/2Z^2\bar{Z}''\right)\beta_0{}^2+\left(i\bar{Z}'ZZ''+iu'Z'+iu''Z+1/2i\bar{Z}'Z'^2+iZ'Z\bar{Z}''-iZ'\bar{Z}Z''\right)\beta_0 \\
& -u'Z''-u''Z'-1/2Z'^2\bar{Z}''-\bar{Z}'Z'Z''\Big]A_{xx}+I_{xx}\Omega_0\varepsilon^2\Big(-i\beta_0\Omega\bar{Z}'+1/4\dot{\bar{Z}}'\beta_0+1/2\Omega\bar{Z}''-1/2\beta_0{}^2\Omega\bar{Z} \\
& +1/4i\dot{\bar{Z}}\beta_0{}^2\Big)e^{-2i(-\beta_0x+\Omega t)}+I_{xx}\Omega_0\varepsilon^2\left(-i\beta_0\Omega\bar{Z}'+1/4\dot{\bar{Z}}'\beta_0-1/2\Omega\bar{Z}''-1/2\beta_0{}^2\Omega\bar{Z}+1/4i\dot{\bar{Z}}\beta_0{}^2\right)e^{2i(\beta_0x+\Omega t)} \\
& +\Big[8\beta_0{}^4\Delta D\bar{Z}-22i\beta_0{}^3\Delta D\bar{Z}'+\left(-21\Delta D\bar{Z}''-6i\Omega_0\Delta I\dot{\bar{Z}}+3\Delta I\ddot{\bar{Z}}\right)\beta_0{}^2+\left(-4i\Delta I\ddot{\bar{Z}}'+8i\Delta D\bar{Z}'''-8\Omega_0\Delta I\dot{\bar{Z}}'\right)\beta_0 \\
& -\Delta I\ddot{\bar{Z}}''+2i\Omega_0\Delta I\dot{\bar{Z}}''+\Delta D\bar{Z}^{(4)}\Big]e^{-2i(\Omega_0t-2\beta_0x)}+\Big[-8\beta_0{}^4\Delta D\bar{Z}-22i\beta_0{}^3\Delta D\bar{Z}'+\left(21\Delta D\bar{Z}''-6i\Omega_0\Delta I\dot{\bar{Z}}-3\Delta I\ddot{\bar{Z}}\right)\beta_0{}^2 \\
& +\left(-4i\Delta I\ddot{\bar{Z}}'+8i\Delta D\bar{Z}'''+8\Omega_0\Delta I\dot{\bar{Z}}'\right)\beta_0+\Delta I\ddot{\bar{Z}}''-2i\Omega_0\Delta I\dot{\bar{Z}}''+\Delta D\bar{Z}^{(4)}\Big]e^{2i(\Omega_0t-2\beta_0x)} \\
& +I_{xx}\Omega_0\varepsilon^2\left(-i\beta_0\Omega Z'-1/4\dot{\bar{Z}}'\beta_0+1/2i\dot{Z}''-1/2\beta_0{}^2\Omega Z-1/4i\dot{Z}\beta_0{}^2-1/2\beta_0{}^2\Omega Z''-3/4\beta_0\dot{Z}'\right)e^{-2i\Omega t} \\
& +I_{xx}\Omega_0\varepsilon^2\left(i\beta_0\Omega Z'-1/4\dot{\bar{Z}}'\beta_0-1/2i\dot{Z}''-1/2\beta_0{}^2\Omega Z+1/4i\dot{Z}\beta_0{}^2+1/2\beta_0{}^2\Omega Z''+3/4\beta_0\dot{Z}'\right)e^{2i\Omega t} \\
& -\frac{I_{xx}\Omega_0}{2}\left[\left(i\beta_0^2\dot{\bar{Z}}-\beta_0\dot{\bar{Z}}'\right)e^{-2i\beta_0x}+\left(-2i\dot{Z}''+3\beta_0\dot{Z}'+i\beta_0^2\dot{Z}\right)\right]=m\Omega_0{}^2\left(e_\eta(x)+ie_\xi(x)\right)e^{-i(\beta_0x-\Omega_0t)}
\end{aligned}
\tag{14}
$$

With boundary conditions: $@x=0,L \quad \Rightarrow \quad u=0, \quad Z=Z''=0$ where

$$
\begin{aligned}
& Z=v+iw, \quad \bar{Z}=v-iw, \quad u=u_\zeta, \quad v=v_\eta, \quad w=w_\xi, \\
& \Delta D=\frac{\left(D_{\xi\xi}-D_{\eta\eta}\right)}{2}, \quad \Delta I=\frac{\left(I_{\xi\xi}-I_{\eta\eta}\right)}{2}, \quad \Sigma D=\frac{\left(D_{\xi\xi}+D_{\eta\eta}\right)}{2}, \quad \Sigma I=\frac{\left(I_{\xi\xi}+I_{\eta\eta}\right)}{2}
\end{aligned}
\tag{15}
$$

Z is the complex form of flexural displacements of v and w. For the slender beams, it can be ignored the inertia term $m\ddot{u}$ from Eq. (13) [41] and using the simply supported boundary conditions, Eq. (13) can be rewritten as,

$$
u'=-\frac{1}{2}\beta_0^2\left(v^2+w^2\right)+\beta_0\left(-vw'+wv'\right)-\frac{1}{2}\left(v'^2+w'^2\right)+\frac{1}{2L}\int_0^L\left(v'^2+w'^2-2\beta_0\left(v'w-vw'\right)+\beta_0^2\left(v^2+w^2\right)\right)dx
\tag{16}
$$

Once again, substituting and simplifying Eq. (16) into Eqs. (13) and (14) and considering orders $v=w=O(\varepsilon)$ and $u=O(\varepsilon^2)$ from the Eq. (16), expanding the resultant equations up to order $O(\varepsilon^3)$, and using the non-dimensional parameters given by,

$$
u^*=\frac{u}{h_0}, v^*=\frac{v}{h_0}, \quad w^*=\frac{w}{h_0}, \quad x^*=\frac{x}{L}, \quad \Omega^*=\frac{\Omega}{\sqrt{\pi^4\text{Ó}D/mL^4}}, \quad \Omega_0^*=\frac{\Omega_0}{\sqrt{\pi^4\text{Ó}D/mL^4}},
$$

$$
t^*=\frac{t}{\sqrt{mL^4/\pi^4\text{Ó}D}}, \mathrm{I}_{xx}^*=\mathrm{I}_{\zeta\zeta}^*=\frac{\pi^2I_{xx}}{mL^2}, \Sigma I^*=\frac{\pi^2\Sigma I}{mL^2}, \qquad c^*=c\frac{\pi^2\sqrt{m\text{Ó}D}}{L^2}, \quad \mu=\frac{h_0^2A_{xx}}{2\Sigma D},
$$

$$
Z^*=v^*+iw^*, \quad \bar{Z}^*=v^*-iw^*
$$

where h_0 is the side of the cross-section of the twisted beam. It should be noted that to avoid the complexity of equations and simplifying them, the asterisk symbol is ignored in the following. So, Complex form of flexural vibration equation is given by,

$$
\begin{aligned}
&\ddot{Z}+\frac{Z^{(4)}}{\pi^4}-\frac{\Sigma I}{\pi^2}\ddot{Z}''-\frac{2i\beta_0^3}{\pi^4}Z'-\frac{\beta_0^2}{\pi^2}\left(-\Sigma I\ddot{Z}+\frac{5}{\pi^2}Z''\right)-\frac{i\beta_0}{\pi^2}\left(2\Sigma I\ddot{Z}'-\frac{4}{\pi^2}Z'''\right)+c\dot{Z}e^{i\beta_0 x}-\frac{\mu}{\pi^4}\Big[iZ'\beta_0^3\int_0^1 Z\bar{Z}dx \\
&+(\bar{Z}'\int_0^1(Z\bar{Z}'-\bar{Z}Z')dx+Z''\int_0^1 Z\bar{Z}dx)\beta_0^2+(Z'\int_0^1 Z'\bar{Z}'dx+iZ''\int_0^1(Z\bar{Z}'-\bar{Z}Z')dx)\beta_0+Z''\int_0^1 Z'\bar{Z}'dx\Big] \\
&+\frac{I_{xx}\Omega_0}{\pi^2}\varepsilon^2\left(-i\beta_0\Omega\bar{Z}'+1/4\dot{\bar{Z}}'\beta_0+1/2\Omega\bar{Z}''-1/2\beta_0^2\Omega\bar{Z}+1/4i\dot{\bar{Z}}\beta_0^2\right)e^{-2i(-\beta_0 x+\Omega t)} \\
&+\frac{I_{xx}\Omega_0}{\pi^2}\varepsilon^2\left(-i\beta_0\Omega\bar{Z}'+1/4\dot{\bar{Z}}'\beta_0-1/2\Omega\bar{Z}''-1/2\beta_0^2\Omega\bar{Z}+1/4i\dot{\bar{Z}}\beta_0^2\right)e^{2i(\beta_0 x+\Omega t)} \\
&+\Big[8\beta_0^4\Delta D\bar{Z}-22i\beta_0^3\Delta D\bar{Z}'+\left(-21\Delta D\bar{Z}''-6i\Omega_0\Delta I\dot{\bar{Z}}+3\Delta I\ddot{\bar{Z}}\right)\beta_0^2+\left(-4i\Delta I\ddot{\bar{Z}}'+8i\Delta D\bar{Z}'''-8\Omega_0\Delta I\dot{\bar{Z}}'\right)\beta_0 \\
&-\Delta I\ddot{\bar{Z}}''+2i\Omega_0\Delta I\dot{\bar{Z}}''+\Delta D\bar{Z}^{(4)}\Big]\frac{e^{-2i(\Omega_0 t-2\beta_0 x)}}{\pi^4}+\Big[-8\beta_0^4\Delta D\bar{Z}-22i\beta_0^3\Delta D\bar{Z}'+\left(21\Delta D\bar{Z}''-6i\Omega_0\Delta I\dot{\bar{Z}}-3\Delta I\ddot{\bar{Z}}\right)\beta_0^2 \\
&+\left(-4i\Delta I\ddot{\bar{Z}}'+8i\Delta D\bar{Z}'''+8\Omega_0\Delta I\dot{\bar{Z}}'\right)\beta_0+\Delta I\ddot{\bar{Z}}''-2i\Omega_0\Delta I\dot{\bar{Z}}''+\Delta D\bar{Z}^{(4)}\Big]\frac{e^{2i(\Omega_0 t-2\beta_0 x)}}{\pi^4} \\
&+\frac{I_{xx}\Omega_0}{\pi^2}\varepsilon^2\left(-i\beta_0\Omega Z'-1/4\dot{\bar{Z}}'\beta_0+1/2i\dot{Z}''-1/2\beta_0^2\Omega Z-1/4i\dot{Z}\beta_0^2-1/2\beta_0^2\Omega Z''-3/4\beta_0\dot{Z}'\right)e^{-2i\Omega t} \\
&+\frac{I_{xx}\Omega_0}{\pi^2}\varepsilon^2\left(i\beta_0\Omega Z'-1/4\dot{\bar{Z}}'\beta_0-1/2i\dot{Z}''-1/2\beta_0^2\Omega Z+1/4i\dot{Z}\beta_0^2+1/2\beta_0^2\Omega Z''+3/4\beta_0\dot{Z}'\right)e^{2i\Omega t} \\
&-\frac{I_{xx}\Omega_0}{2\pi^2}\left[\left(i\beta_0^2\dot{\bar{Z}}-\beta_0\dot{\bar{Z}}'\right)e^{-2i\beta_0 x}+\left(-2i\dot{Z}''+3\beta_0\dot{Z}'+i\beta_0^2\dot{Z}\right)\right]=\Omega_0^2\left(e_\eta(x)+ie_\xi(x)\right)e^{-i(\beta_0 x-\Omega_0 t)}
\end{aligned}
\tag{17}
$$

where h_0 is the side of the cross-section of the twisted beam. It should be noted that to avoid the complexity of equations and simplifying them, the asterisk symbol is ignored in the following. Here, to analyze the above equation of motions, Galerkin's methods and multiple scales are utilized to extract the solution of the system. In this procedure, the partial differential equations of motion are converted to the Ordinary Differential Equations (ODEs) by Galerkin's method and stability of the system is analyzed by multiple scales method. Also, the results are obtained numerically by Runge-Kutta method and finally, both of obtained results validated together.

3. SOLUTION METHOD

In this section, the multiple scales method after discretization by the Galerkin's procedure is applied to analyze the transverse parametric resonances due to the asymmetry and spinning speed fluctuation. Furthermore, in this study, it has been assumed that the twisted beam is driven near the natural frequency of the linear mode and that the mode is not involved an internal resonance with other modes. So, the response is usually referred to a single-mode approximation [42]. A single mode Galerkin method may be used to discretize the nonlinear coupled partial differential equation, Eq. (17), as following [42, 43],

$$Z(x,t)=\Phi_n(x)Z(t) \tag{18}$$

where n is the mode number and $\Phi_n(x)$ is the linear transverse mode shape which is

$$\Phi_n(x)=\sin(n\pi x) \tag{19}$$

Substituting Eqs. (18) and (19) into Eq. (17), multiplying the equation by its corresponding mode shape, integrating by parts over the interval [0,1] and using the orthogonality of mode shapes leads to,

$$
\begin{aligned}
&i\left(\Pi_{6,v}\ddot{\bar{Z}}+\Pi_{7,v}\dot{\bar{Z}}-\Pi_{8,v}\bar{Z}\right)\left(\frac{e^{i(-2\Omega_0 t+4\beta_0)}-e^{(2i\Omega_0 t)}}{\beta_0}\right)+1/2i\varepsilon^2\Pi_{1,v}\dot{Z}\left(e^{(-2i\Omega t)}+e^{(2i\Omega t)}\right) \\
&+1/4\varepsilon^2 I_{xx}\Omega_0\Omega\Big[1/2\left(2i\Pi_{5,v}\bar{Z}+\Pi_{3,v}Z\right)e^{(2i\Omega t)}+1/2\left(2i\Pi_{5,v}\bar{Z}-\Pi_{3,v}Z\right)e^{(-2i\Omega t)}+i\Pi_{5,v}\bar{Z}e^{2i(\Omega t-\beta_0)}\Big] \\
&+i\Pi_{1,v}\dot{Z}-\Pi_{4,v}c(\frac{1+e^{i\beta_0}}{\beta_0})\dot{Z}+1/2\Pi_{2,v}\ddot{Z}+\Pi_{3,v}\mu Z^2\bar{Z}+2\Pi_{9,v}Z+1/4\Pi_{5,v}\Omega_0^2\left(e_\eta+ie_\xi\right)e^{(i\Omega_0 t)}=0
\end{aligned}
\tag{20}
$$

Where

$$\Pi_{1,v} = \left(8\beta_0^6 - 18\pi^2 n^2 \beta_0^4 - 60\pi^4 n^4 \beta_0^2 + 16\pi^6 n^6\right) I_{xx}\Omega_0,$$
$$\Pi_{2,v} = \Big[136\pi^4 n^2 \beta_0^2 - 32\left(\pi^4 n^4 + \pi^2 \beta_0^4\right) - 32\left(\pi^6 n^6 + \beta_0^6\right)$$
$$\Sigma I + 104\pi^2 n^2 \beta_0^2 \left(\pi^2 n^2 + \beta_0^2\right)\Sigma I\Big],$$
$$\Pi_{3,v} = \left[208\pi^2 n^4 \beta_0^2 \left(\pi^2 n^2 + \beta_0^2\right) - 64\left(\pi^6 n^8 + n^2 \beta_0^6\right)\right],$$
$$\Pi_{4,v} = 16\pi^4 n^2 \left(\pi^2 n^2 - 4\beta_0^2\right), \Pi_{5,v} = \tag{21}$$
$$4\left(-17\beta_0^2 n^2 \pi^4 + 4\pi^2 \beta_0^4 + 4n^4 \pi^6\right)$$
$$\Pi_{6,v} = \left(21\pi^2 n^2 \beta_0^2 - 4\pi^4 n^4 - 5\beta_0^4\right)\pi^2 n^2 \Delta I, \Pi_{7,v} =$$
$$\left(-42\pi^2 n^2 \beta_0^2 + 8\pi^4 n^4 + 10\beta_0^4\right)\pi^2 n^2 \Delta I\,\Omega_0,$$
$$\Pi_{8,v} = \left(4\pi^6 n^8 + 36\beta_0^6 n^2 + 19\pi^4 n^6 \beta_0^2 - 149\pi^2 n^4 \beta_0^4\right)\Delta D,$$
$$\Pi_{9,v} = \left[-6\pi^4 n^4 \beta_0^2 - 8\pi^6 n^6 + 162\beta_0^4 n^2 \pi^2 - 40\beta_0^6\right] n^2 \pi^2,$$
$$e_\eta = \int_0^1 \frac{\Phi_{f|b}(x)}{e^{i\beta_0 x}} e_\eta(x)dx, \quad e_\xi = \int_0^1 \frac{\Phi_{f|b}(x)}{e^{i\beta_0 x}} e_\xi(x)dx.$$

Since the Eq. (20) has cubic nonlinearities, transverse component of $Z(t) = v(t) + iw(t)$ is expressed as following [42, 43],

$$Z(t) = \varepsilon Z_1(T_0, T_2) + \varepsilon^3 Z_3(T_0, T_2) + \ldots \tag{22}$$

where ε is the small parameter which can be used as a book keeping parameter and $T_n = t$ and $T_2 = \varepsilon^2 t$. Hence, time derivatives can be recomputed using the chain rule as following,

$$\frac{\partial}{\partial t} = D_0 + \varepsilon^2 D_2 + \ldots \text{ and } \frac{\partial^2}{\partial t^2} = D_0{}^2 + 2\varepsilon^2 D_2 D_0 + \ldots \tag{23}$$

where $D_n = \partial / \partial T_n$. To obtain the primary and parametric resonances and balance the nonlinearities, the parameters c, ΔD, ΔI, e_ξ and e_η are written as following,

$$c = \varepsilon^2 c, \quad \Delta D = \varepsilon^2 \Delta D, \quad \Delta I = \varepsilon^2 \Delta I, \quad e_\eta = \varepsilon^3 e_\eta, \quad e_\xi = \varepsilon^3 e_\xi \tag{24}$$

Substituting the Eqs. (22) to (24) into Eq. (20) and equating coefficients of like power of ε yields,

$O(\varepsilon)$:

$$2\Pi_{9,v} Z_1 + 1/2 D_0^2 Z_1 + i\Pi_{1,v} D_0 Z_1 = 0 \tag{25}$$

And

$O(\varepsilon^3)$:

$$i\Pi_{1,v} D_0 Z_3 + 1/2 D_0^2 \Pi_{2,v} Z_3 + 2\Pi_{9,v} Z_3$$
$$+\Pi_{2,v} D_2 D_0 Z_1 + i\Pi_{1,v} D_2 Z_1 + \Pi_{3,v} \mu Z_1{}^2 \bar{Z}_1$$
$$+i\left(\Pi_{6,v} D_0^2 \bar{Z}_1 + \Pi_{7,v} D_0 \bar{Z}_1 - \Pi_{8,v} \bar{Z}_1\right)$$
$$\left(\frac{e^{i(-2\Omega_0 T_0 + 4\beta_0)} - e^{(2i\Omega_0 T_0)}}{\beta_0}\right) + 1/2 i\Pi_{1,v} D_0 Z_1$$
$$\left(e^{(-2i\Omega T_0)} + e^{(2i\Omega T_0)}\right) \tag{26}$$
$$+1/4 I_{xx}\,\Omega_0 \Omega \begin{bmatrix} 1/2\left(-2i\Pi_{5,v}\bar{Z}_1 + \Pi_{3,v} Z_1\right) \\ e^{(2i\Omega T_0)} + 1/2\left(2i\Pi_{5,v}\bar{Z}_1 - \Pi_{3,v} Z_1\right) \\ e^{(-2i\Omega T_0)} + i\Pi_{5,v}\bar{Z}_1 e^{2i(\Omega T_0 - \beta_0)} \end{bmatrix}$$
$$-\Pi_{4,v} c\left(\frac{1 + e^{i\beta_0}}{\beta_0}\right) D_0 Z_1 + 1/4 \Pi_{5,v} \Omega_0{}^2 \left(e_\eta + ie_\xi\right) e^{(i\Omega_0 T_0)} = 0$$

The general solution of Eq. (25) is,

$$Z_1(T_0, T_2) = A_1(T_2) e^{i\omega_f T_0} + A_2(T_2) e^{i\omega_b T_0} \tag{27}$$

where ω_f and ω_b denote to the linear forward and backward frequencies, which for the simply supported beam with speed fluctuation are given by [40],

$$\omega_{f,b} = \frac{1}{2}\frac{\delta_1 \pm \sqrt{\delta_3}}{\delta_2} \tag{28}$$

where

$$\delta_1 = I_{xx}\Omega_0(\beta 0^2 + 2\pi^2 n^2) \quad ,$$

$$\delta_2 = 2\left(\pi^2 + \left(\pi^2 n^2 + \beta_0^2\right)\Sigma I\right)$$

$$\delta_3 = \left(I_{xx}\Omega_0 \beta_0^2\right)^2 + 4\begin{bmatrix} 4\pi^4 n^6 \Sigma I + 4\pi^4 n^4 + \left(I_{xx}\Omega_0 \pi n \beta_0\right)^2 \\ +\left(I_{xx}\Omega_0 \pi^2 n^2\right)^2 + 24\Sigma I(\beta_0 \pi n^2)^2 + \\ 20(\pi n \beta_0)^2 + 20\Sigma I(\beta_0^2 n)^2 \end{bmatrix}$$

And $A_1(T_2)$ and $A_2(T_2)$ are complex amplitudes of the forward and backward whirling, respectively. To analyze the primary and parametric resonances, nearness Ω to Ω_0 and ω_f can be indicated by detuning parameters σ_1 and σ_2 as following [43],

$$\Omega = \omega_f + \varepsilon^2 \sigma_1, \quad \Omega_0 = \omega_f + \varepsilon^2 \sigma_2 \tag{29}$$

where $\sigma_1 = \sigma_2 = O(1)$ [43]. Substituting Eqs. (27) to (29) into Eq. (26) leads to

$$\begin{aligned} & i\Pi_{1,v} D_0 Z_3 + 1/2 D_0^2 \Pi_{2,v} Z_3 + 2\Pi_{9,v} Z_3 \\ & = G_f(T_2) e^{i\ \ _f T_0} + G_b(T_2) e^{i\ \ _b T_0} + N.S.T + CC \end{aligned} \tag{30}$$

where CC and $N.S.T$ denote to the complex conjugate and non-secular terms. Also,

$$\begin{aligned} & G_f(T_2) = G_{f,v}(T_2) + iG_{f,w}(T_2) \text{ and} \\ & G_b(T_2) = G_{b,v}(T_2) + iG_{b,w}(T_2) \end{aligned} \tag{31}$$

$G_{f,v}(T_2)$, $G_{b,v}(T_2)$, $G_{f,w}(T_2)$, and $G_{b,w}(T_2)$ include the secular terms and are given in the Appendix A. To obtain the solvability conditions, the secular terms must be eliminated. Hence, particular solutions corresponding to the $\pm e^{i\omega_f T_0}$ and $\pm e^{i\omega_b T_0}$ in Eq. (30) are,

$$\begin{aligned} & Z_3(T_0, T_2) = \left[P_{11}(T_2) + iP_{22}(T_2)\right] e^{i\omega_f T_0} \\ & + \left[Q_{11}(T_2) + iQ_{22}(T_2)\right] e^{i\omega_b T_0} \end{aligned} \tag{32}$$

Substituting Eq. (32) into Eq. (30) and equating the coefficients of each of $\pm e^{i\omega_f T_0}$ and $\pm e^{i\omega_b T_0}$, it can clearly be seen that the Eq. (30) has a non-trivial solution. So, its solvability conditions can be written as,

$$\begin{aligned} & \begin{vmatrix} -1/2\Pi_{2,v}\omega_f^2 + 2\Pi_{9,v} & G_{f,v} \\ i\Pi_{1,v}\omega_f & G_{f,w} \end{vmatrix} = 0 \quad \text{or} \\ & \begin{vmatrix} G_{f,v} & -i\Pi_{1,v}\omega_f \\ G_{f,w} & -1/2\Pi_{2,v}\omega_f^2 + 2\Pi_{9,v} \end{vmatrix} = 0 \end{aligned} \tag{33}$$

And

$$\begin{aligned} & \begin{vmatrix} -1/2\Pi_{2,v}\omega_b^2 + 2\Pi_{9,v} & G_{b,v} \\ i\Pi_{1,v}\omega_b & G_{b,w} \end{vmatrix} = 0 \quad \text{or} \\ & \begin{vmatrix} G_{b,v} & -i\Pi_{1,v}\omega_b \\ G_{b,w} & -1/2\Pi_{2,v}\omega_b^2 + 2\Pi_{9,v} \end{vmatrix} = 0 \end{aligned} \tag{34}$$

Simplifying the Eqs. (33) and (34) gives two equations as following,

$$\begin{aligned} & i\left[\Pi_{1,v} + \Pi_{2,v}\omega_f\right] D_2 A_1 + 4\mu\Pi_{3,v} {A_1}^2 \bar{A}_1 \\ & + \Pi_{4,v} c\omega_f \left(\frac{1 - e^{i\beta_0}}{\beta_0}\right) A_1 + 2\mu\Pi_{3,v} A_1 \bar{A}_2 A_2 \\ & + \left[\Gamma 2 \left(\frac{1\text{-}e^{-4i\beta_0}}{\beta_0}\right) + \Gamma 1 \left(1 + e^{-2i\beta_0}\right)\right] e^{2i\sigma T_2} \bar{A}_1 \\ & + \Pi_{5,v}\left(e_\eta + ie_\xi\right) {\Omega_0}^2 e^{i\sigma T_2} = 0 \end{aligned} \tag{35}$$

And

$$\begin{aligned} & i\Pi_{1,w} D_2 A_2 + 16 n^2 \pi^2 c\omega_b \left(\frac{1 - e^{i\beta_0}}{\beta_0}\right) A_2 \\ & + \Pi_{2,w} \mu \bar{A}_2 {A_2}^2 + 2\Pi_{2,w} \mu A_2 A_1 \bar{A}_1 = 0 \end{aligned} \tag{36}$$

where $\overline{A_1}$ and $\overline{A_2}$ are complex conjugates of A_1 and A_2, respectively and,

$$\begin{aligned} & \Pi_{1,w} = \Big[2\left(-\beta_0^4 + 2\beta_0^2 n^2 \pi^2 + 8n^4\pi^4\right) I_{xx}\Omega_0 \\ & + 8\left(-3\beta_0^2 n^2\pi^2 + \beta_0^4 - 4n^4\pi^4\right) \Sigma I\,\omega_b, \\ & + 8\left(-4n^2\pi^4 + \pi^2\beta_0^2\right)\omega_b\Big], \Pi_{2,w} \\ & = 16\left(n^2\beta_0^4 - 3\beta_0^2 n^4\pi^2 - 4n^6\pi^4\right), \\ & \Gamma 1 = 1/4\Pi_{5,v} I_{xx} {\Omega_0}^2 n^2, \quad \Gamma 2 \\ & = \Pi_{6,v}\omega_f^2 + \Pi_{7,v}\omega_f + \Pi_{8,v} \end{aligned} \tag{37}$$

As shown in Eqs. (35) to (37), $\Gamma 1$ and $\Gamma 2$ denote to the speed fluctuation and asymmetry terms which are the coefficients of $e^{2i\sigma T_2}$. This means that asymmetry and speed fluctuation effects lead to the parametric resonances with frequency 2Ω. To extend and simplify the solutions of the Eqs. (35) and (36), $e^{i\sigma T_2}$ is eliminated by converting $A_1(T_2)$ and $A(T_2)$ as

$$A_1(T_2) = A(T_2) e^{i\sigma T_2} \tag{38}$$

Then, $A(T_2)$ and $A_2(T_2)$ are expressed as the polar forms

$$A(T_2) = \frac{1}{2} a_1(T_2) e^{i\Theta(T_2)}, A_2(T_2) = \frac{1}{2} a_2(T_2) e^{i\theta(T_2)} \tag{39}$$

where $a_1(T_2)$ and $a_2(T_2)$ are the amplitudes and $\Theta(T_2)$ and $\theta(T_2)$ are phase angles of the forward and backward whirling, respectively. Substituting the Eq. (39) into the resultant Equations, simplifying and separating the real and imaginary parts, four first-order modulation equations are obtained as following,

$$\begin{aligned} & \left[\Pi_{1,v} + \Pi_{2,v}\omega_f\right] a_1 D_2 \Theta = 1/4\Pi_{3,v}\mu {a_1}^3 \\ & + \Pi_{4,v}\left(\frac{1 - \cos(\beta_0)}{\beta_0}\right) c\omega_f a_1 + 1/2\Pi_{3,v}\mu {a_2}^2 a_1 \\ & + \begin{bmatrix} \Gamma 2 \left(\dfrac{\sin(2\Theta) - \sin(4\beta_0 + 2\Theta)}{\beta_0}\right) \\ + \Gamma 1 \left(\dfrac{\sin(2\Theta) - \sin(2\Theta + 2\beta_0)}{\beta_0}\right) \end{bmatrix} a_1 \\ & - \left[\Pi_{1,v} + \Pi_{2,v}\omega_f\right] \sigma a_1 + 2\Omega_0^2 \Pi_{5,v} \\ & \left(e_\xi \sin(\Theta) + e_\eta \cos(\Theta)\right) \end{aligned} \tag{40}$$

$$\left[\Pi_{1,v}+\Pi_{2,v}\omega_f\right]D_2a_1=\begin{bmatrix}\Gamma 2\left(\dfrac{-\cos(2\Theta)+\cos(4\beta_0+2\Theta)}{\beta_0}\right)\\+\Gamma 1\left(\dfrac{-\cos(2\Theta)+\cos(2\Theta+2\beta_0)}{\beta_0}\right)\end{bmatrix}a_1$$

(41)

$$+\Pi_{4,v}\sin(\beta_0)c\omega_f a_1+2\Pi_{5,v}\Omega_0^2\left(e_\eta\sin(\Theta)-e_\xi\cos(\Theta)\right)$$

$$\Pi_{1,w}D_2a_2=16n^2\pi^4c\,\omega_b\left(\frac{\sin(\beta_0)}{\beta_0}\right)a_2 \tag{42}$$

$$\frac{1}{2}\Pi_{1,w}a_2D_2\theta=\frac{1}{2}\Pi_{2,w}\mu a_2a_1^2$$
$$+8n^2\pi^4c\,\omega_b\left(\frac{1-\cos(\beta_0)}{\beta_0}\right)a_2+\frac{1}{8}\Pi_{2,w}\mu a_2^{\,3} \tag{43}$$

Because the amplitudes and phases are not change at an equilibrium solution, the steady state responses of the system occur at this solution. Consequently, to analyze the equilibrium solutions, time derivatives are equated with zero and according to the Eqs. (42) and (43), a_2 will be zero. This means that in the simultaneous resonances of nonlinear gyroscopic asymmetrical twisted beam with speed fluctuations, the effect of backward mode is negligible and vibration modes are only a function of the forward whirling. Hence, the following equations can be obtained,

$$1/4\Pi_{3,v}\mu a_{10}^{\;3}-\left[\Pi_{1,v}+\Pi_{2,v}\omega_f\right]\sigma a_{10}$$
$$+\begin{bmatrix}\Gamma 2\left(\dfrac{\sin(2\Theta_0)-\sin(4\beta_0+2\Theta_0)}{\beta_0}\right)\\+\Gamma 1\left(\dfrac{\sin(2\Theta_0)-\sin(2\Theta_0+2\beta_0)}{\beta_0}\right)\end{bmatrix}a_{10}$$
$$+\Pi_{4,v}\left(\frac{1-\cos(\beta_0)}{\beta_0}\right)c\omega_f a_{10}+2\Omega_0^2\Pi_{5,v}$$
$$\left(e_\xi\sin(\Theta_0)+e_\eta\cos(\Theta_0)\right)=0 \tag{44}$$

$$\Pi_{4,v}\sin(\beta_0)c\omega_f a_{10}+\begin{bmatrix}\Gamma 2\left(\dfrac{-\cos(2\Theta_0)+\cos(4\beta_0+2\Theta_0)}{\beta_0}\right)\\+\Gamma 1\left(\dfrac{-\cos(2\Theta_0)+\cos(2\Theta_0+2\beta_0)}{\beta_0}\right)\end{bmatrix}a_{10}$$
$$+2\Pi_{5,v}\Omega_0^2\left(e_\eta\sin(\Theta_0)-e_\xi\cos(\Theta_0)\right)=0 \tag{45}$$

where a_{10} and Θ_0 are the equilibrium solutions (steady solutions) of Eqs. (40) and (41).

4. STABILITY ANALYSIS

The stability of the steady-state motion is investigated by the eigenvalues of the Jacobian matrix of the right hand sides of Eqs. (40) and (41) [44].

$$J=\begin{bmatrix}A & B\\ C & D\end{bmatrix} \tag{46}$$

where

$$A=\frac{3\Pi_{3,v}}{4\Lambda_{1,v}a_{10}}\mu a_{10}^2+\frac{\Pi_{4,v}}{\Lambda_{1,v}a_{10}}\left(\frac{1-\cos(\beta_0)}{\beta_0}\right)c\omega_f-\frac{\sigma}{a_{10}}$$
$$+\frac{1}{\Lambda_{1,v}a_{10}}\begin{bmatrix}\Gamma 1\left(\dfrac{\sin(2\Theta_0)-\sin(2\Theta_0+2\beta_0)}{\beta_0}\right)\\+\Gamma 2\left(\dfrac{\sin(2\Theta_0)-\sin(4\beta_0+2\Theta_0)}{\beta_0}\right)\end{bmatrix}$$

$$B=\frac{2}{\Lambda_{1,v}}\begin{bmatrix}\Gamma 2\left(\dfrac{\cos(2\Theta_0)-\cos(4\beta_0+2\Theta_0)}{\beta_0}\right)\\+\Gamma 1\left(\dfrac{\cos(2\Theta_0)-\cos(2\Theta_0+2\beta_0)}{\beta_0}\right)\end{bmatrix}$$
$$+2\Omega_0^{\,2}\frac{\Pi_{5,v}}{\Lambda_{1,v}a_{10}}\left(e_\xi\cos(\Theta_0)-e_\eta\sin(\Theta_0)\right)$$

$$C=\frac{1}{\Lambda_{1,v}}\begin{bmatrix}\Gamma 2\left(\dfrac{-\cos(2\Theta_0)+\cos(4\beta_0+2\Theta_0)}{\beta_0}\right)\\+\Gamma 1\left(\dfrac{-\cos(2\Theta_0)+\cos(2\Theta_0+2\beta_0)}{\beta_0}\right)\end{bmatrix}$$

$$+\frac{\Pi_{4,v}}{\Lambda_{1,v}}\sin(\beta_0)c\omega_f$$

$$D=\frac{2}{\Lambda_{1,v}}\begin{bmatrix}\Gamma 2\left(\dfrac{2\sin(2\Theta_0)-2\sin(4\beta_0+2\Theta_0)}{\beta_0}\right)\\+\Gamma 1\left(\dfrac{\sin(2\Theta_0)-\sin(2\Theta_0+2\beta_0)}{\beta_0}\right)\end{bmatrix}a_{10}$$
$$+2\Omega_0^{\,2}\frac{\Pi_{5,v}}{\Lambda_{1,v}}\left(e_\eta\cos(\Theta_0)+e_\xi\sin(\Theta_0)\right)$$

And its corresponding eigenvalues is checked as following,

$$\left|J-\lambda_i I\right|=0 \quad \text{or} \quad \lambda_i^2-(A+D)\lambda_i+AD-BC=0 \tag{47}$$

From the Eqs. (46) and (47), the steady-state motion is stable for the equilibrium solutions (a_{10},Θ_0), when $AD-BC>0$ and unstable when $AD-BC<0$.

5. RESULTS AND DISCUSSION

Here, the analytical and numerical results due to the imbalance, asymmetry and spinning speed fluctuation on the

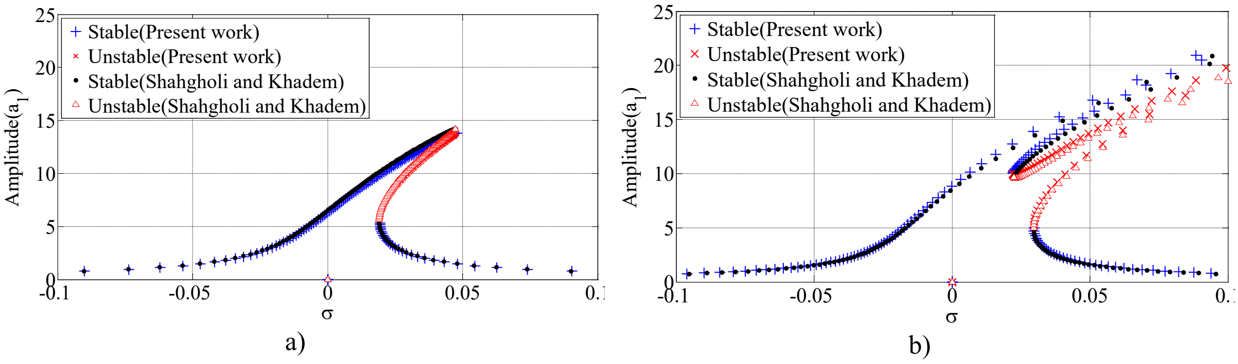

Fig. 2. Comparison of frequency response curves of a straight symmetrical beam ($\Gamma 2=0$) in present work (for $\beta_0=0$) and work of Shahgholi and Khadem [45]. First mode and a) without the speed fluctuation ($\Gamma 1=0$) and b) with the speed fluctuation ($\Gamma 1 \neq 0$).

spinning pre-twisted beam with simply support boundary conditions are investigated. Influences of the speed fluctuation, damping ratio, eccentricity and mass moment of inertia about the x-axis in the different twist angles, natural frequencies and stability domains are investigated. As shown in the previous section, all of the parameters are dimensionless. Here, considered numerical values are, $I_{xx}=0.001$, $I_{\xi\xi}$=0.003275, $I_{\eta\eta}=0.002878$, values are, $I_{xx}=0.001$, $I_{\xi\xi}$=0.003275, $I_{\eta\eta}=0.002878$, $\mu=0.0005$, $c=0.01$, $e_\eta=e_\xi=0.05$.

The first validation for the obtained results is done by equating $\beta_0=0$ into Eqs. (40) and (41) so that the twisted beam is converted to an untwisted beam with and without the spinning speed fluctuation and its frequency responses in the first mode are plotted in Figs. 2(a) and 2(b). Once again, the corresponding curves are extracted from reference [45] and both of the curves have been plotted in Figs. 2(a) and 2(b) with and without the speed fluctuation in first mode and symmetrical cross section. Comparison of these curves is showing a good correlation together. But, as shown in Fig. 2(b) for the present work, since two obtained branches are near together, it can be said that the influence of speed fluctuation is negligible in the first mode. Consequently, according to reference [45], it can be said that there is a single peak and a jump occur.

Figs. 3 and 4 show frequency response curves of the spinning asymmetrical twisted beam with and without the spinning speed fluctuation for first two modes. Assuming that the eccentricities are the same in two principle directions, i.e. $e_\eta=e_\xi=0.05$, from the Eq. (35), it is observed that there are three excitation sources in case of the asymmetrical beam with speed fluctuation, one of which is due to the imbalance with the excitation frequency Ω and second and third excitation sources are due to the asymmetry and speed fluctuation of the beam with the frequency 2Ω. These two excitation sources are parametric excitations and the previous works shown that in presence of the asymmetry and speed fluctuation in straight beams, frequency response curves have two peaks and are bent toward the right direction [40-45]. Hence the nonlinearity effects are of hardening type. However, in present work, it is shown when the beam is a twisted beam; trend of the frequency responses is similar to the straight beams. Also, for some values σ, there are five solutions which two

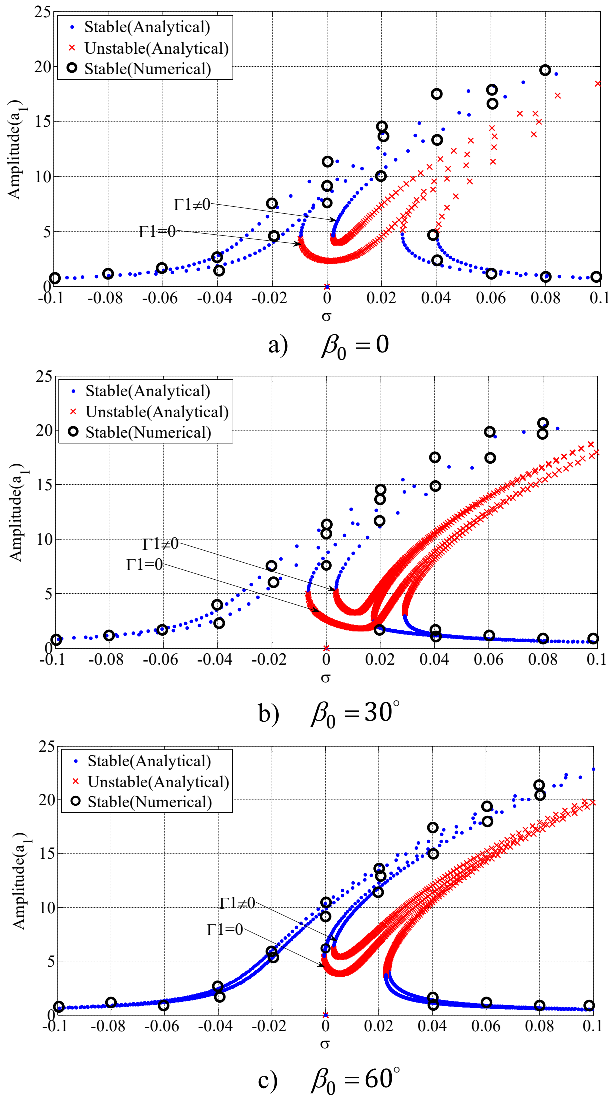

Fig. 3. Frequency response curve of the asymmetrical pre-twisted beam for first mode and different twist angles.

solutions are unstable and three solutions are stable. There are three solutions, for some values σ, one of which is unstable and the rest are stable. Finally, for some values σ, there is a single stable solution. Hence, it is clear that there are jump phenomena and bifurcation points occur with and without the speed fluctuation. In the reference [45] for straight beam and the lower modes, in presence of the asymmetry and speed fluctuation, it is reported that influence of the asymmetry is dominant. However, for twisted beam, as shown in Figs. 3 and 4, although the effect of speed fluctuation is weak in the lower modes, but with increasing the twist angle this effect is amplified. For example, in $\beta_0 = 60^\circ$, frequency response curves with the speed fluctuation ($\Gamma 1 \neq 0$) approach to the frequency response curves without the speed fluctuation ($\Gamma 1 = 0$). In other words, in lower modes, speed fluctuation excitation source can help to pump energy to the system in the larger twist angles while in smaller twist angles, generally, asymmetry pumps energy to the system. Also, ascending the mode number increases speed fluctuation effects. Moreover, validating the analytical results obtained from the perturbation method is done with the numerical results obtained from the Runge-Kutta method. These results have been depicted in Figs. 3 and 4 and are compatible together.

Figs. 5 and 6 give the curve of the amplitude versus the damping ratio of the asymmetrical spinning pre-twisted beam for the different twist angles, first two modes, in presence or absence of the spinning speed fluctuation and the natural frequency corresponding to $\sigma = 0$. As shown in first mode, in the case of the asymmetrical pre-twisted beam ($\Gamma 2 \neq 0$) and in presence of the speed fluctuation ($\Gamma 1 \neq 0$), there is a single stable solution in all of the twisted angles while in the absence of the speed fluctuation ($\Gamma 1 = 0$), there are three solutions which two of them are stable and the other is unstable. So, at the any twist angle with speed fluctuation ($\Gamma 1 \neq 0$), bifurcation do not occur whereas in the absence of speed fluctuation ($\Gamma 1 = 0$), bifurcation occurs. Also, ascending the damping coefficient decreases stable amplitude at the any twist angle with and without the speed fluctuation.

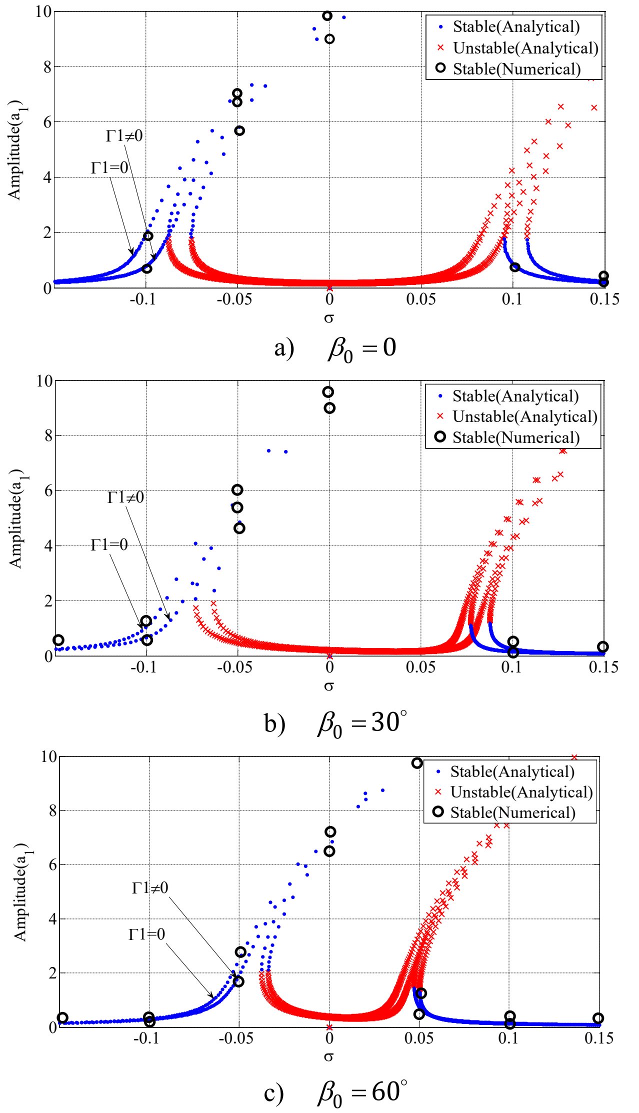

Fig. 4. Frequency response curve of the asymmetrical pre-twisted beam for second mode and different twist angles.

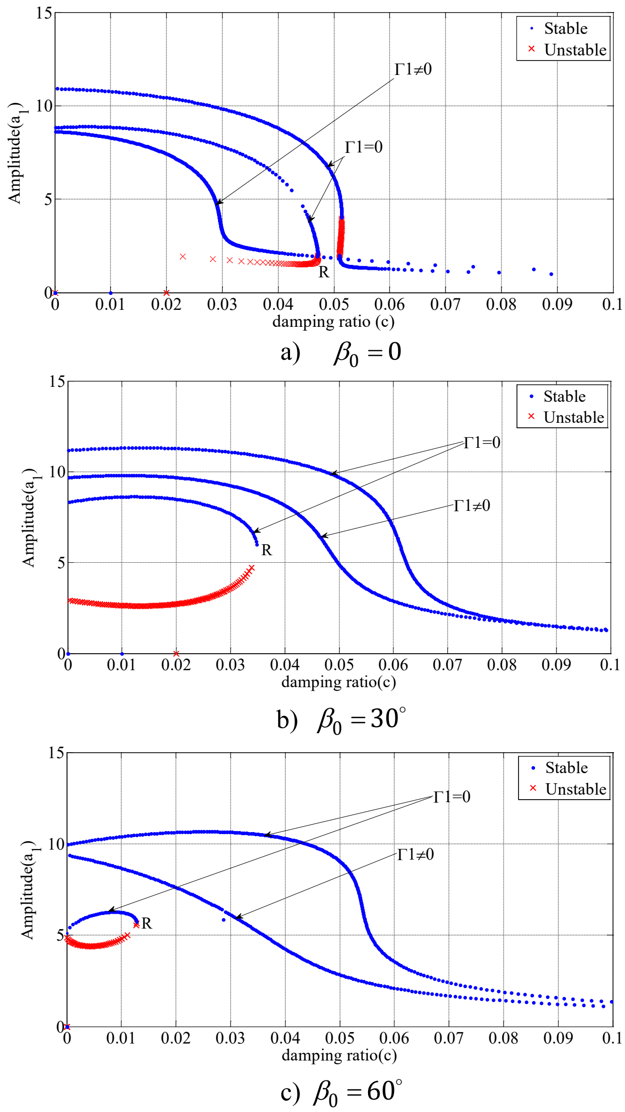

Fig. 5. Curve of the amplitude-damping ratio of the asymmetrical pre-twisted beam for different twist angles, first mode, $\sigma = 0$ and $e_\eta = e_\xi = 0.05$.

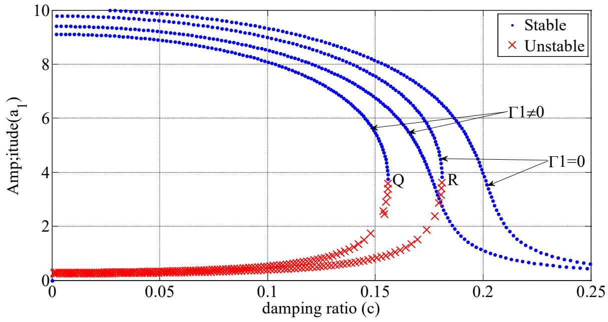

a) $\beta_0 = 0$

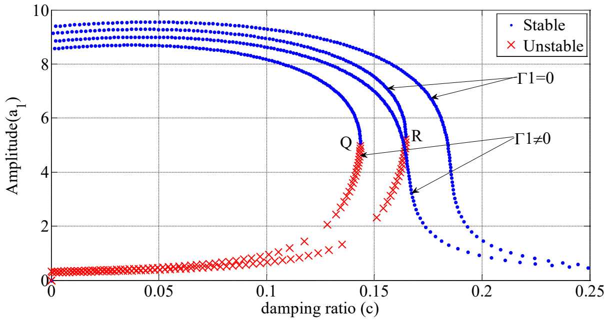

b) $\beta_0 = 30^{\circ}$

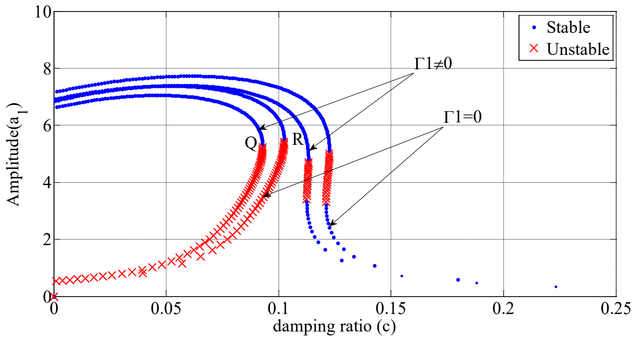

c) $\beta_0 = 60^{\circ}$

Fig.6. Curve of the amplitude-damping ratio of the asymmetrical pre-twisted beam for different twist angles, second mode, $\sigma = 0$ and $e_\eta = e_\xi = 0.05$.

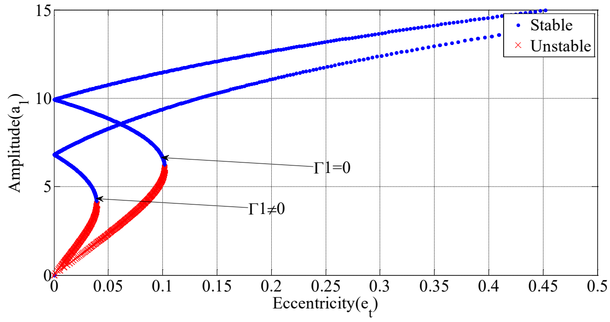

a) $\beta_0 = 0$

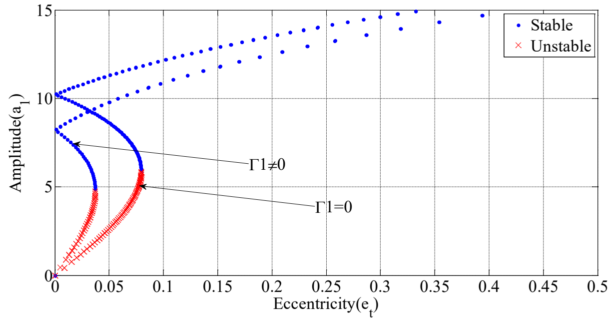

b) $\beta_0 = 30^{\circ}$

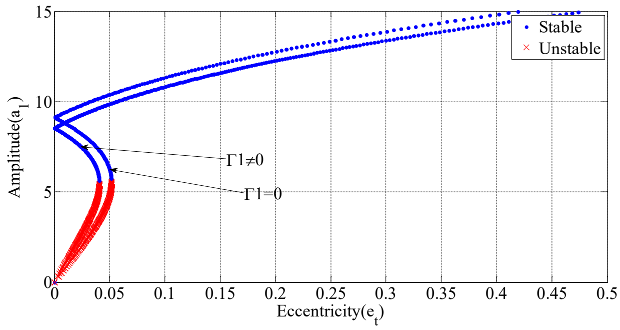

c) $\beta_0 = 60^{\circ}$

Fig. 7. Curve of the amplitude-eccentricity of the asymmetrical pre-twisted beam for different twist angles, first mode and $\sigma = 0$.

More important result is that ascending the twist angle in the asymmetrical twisted beam without the speed fluctuation is caused bifurcation point or jump point (point '***R***') occur in the smaller damping ratio and bifurcation is gradually eliminate and the system will have a single stable solution in over the damping ratios. In presence of the speed fluctuation, the conditions are similar to case without the speed fluctuation. In this case, ascending the twist angle makes the gradient of the amplitude versus damping ratio is more and stable oscillation amplitude is quickly damped. In second mode and for both of the cases (in presence and absence the speed fluctuation), there are three solutions in smaller damping ratios and any twist angle which two of them are stable and the other is unstable; Hence there is bifurcation point (point '***R***' in presence of the speed fluctuation and point '***Q***' in absence of the speed fluctuation). As shown in Fig. 6, in presence and absence of the speed fluctuation, ascending the twist angle shifts these bifurcation points toward the left direction and jump occur in smaller damping ratios. Comparison of these curves in first and second modes indicates that the speed fluctuation effect is more in the second mode and ascending the twist angle makes these curves near together in presence and absence of the speed fluctuation. In the other words, speed fluctuation effect is considerable by ascending the mode numbers and twist angles.

Figs. 7(a-c) and 8(a-c) show the influences of twist angle (β_0) on the amplitude-eccentricity curve of the asymmetrical twisted beam for first two modes and near the natural frequency corresponding to $\sigma = 0$ in presence ($\Gamma 1 \neq 0$) and absence of the speed fluctuation ($\Gamma 1 = 0$). As seen, the oscillation motion of the spinning twisted beam with and without the speed fluctuation has three solutions which two of

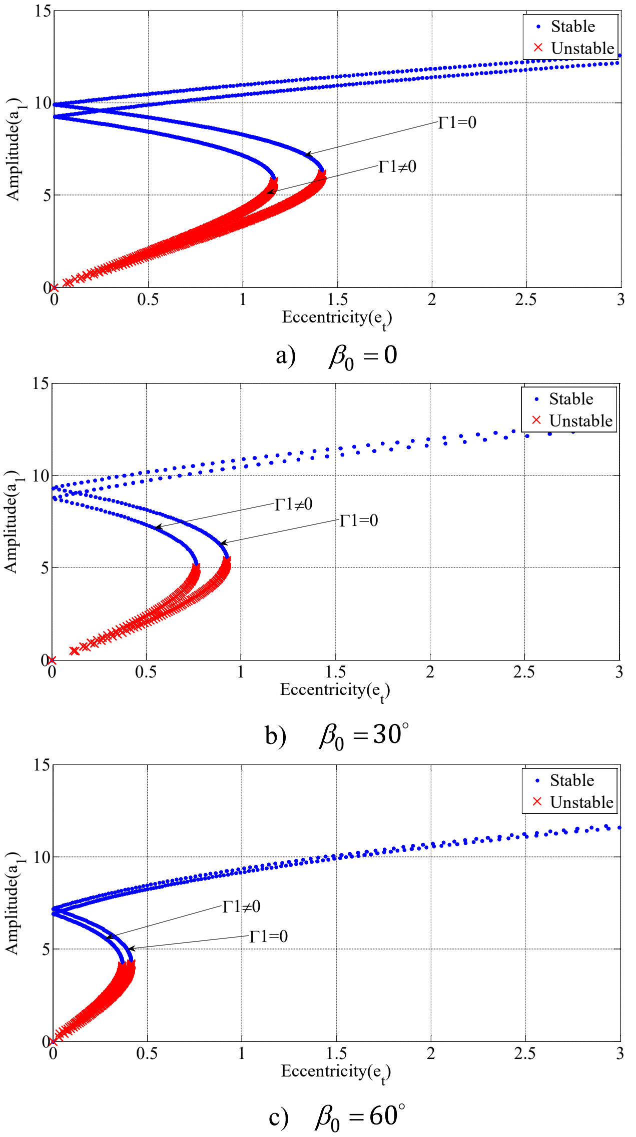

Fig. 8. Curve of the amplitude-eccentricity of the asymmetrical pre-twisted beam for different twist angles, second mode and $\sigma = 0$.

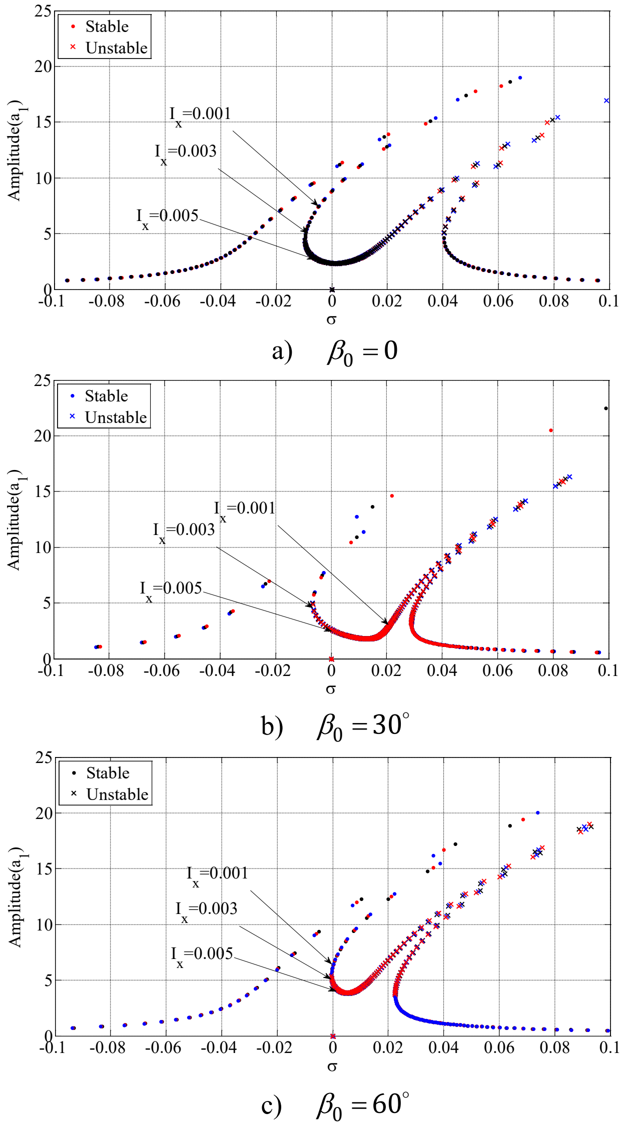

Fig. 9. Influence of the moment of inertia about the x –axis on the frequency response curve of the asymmetrical pre-twisted beam without the speed fluctuation in first mode and different twist angles.

them are stable and the other is unstable. Consequently, jump and bifurcation phenomena occur. Furthermore, as shown in Figs. 7 and 8, in lower modes, speed fluctuation effect is weak and descending the amplitude while asymmetrical effect is dominant. But, in any

mode, ascending the twist angle amplifies speed fluctuation effect so that curves with speed fluctuation are approached to the curves without the speed fluctuation. This fact is more considerable in larger modes.

Figs. 9 and 10 show influence of the moment of inertia about the x-axis (I_{xx}) of the twisted beam on the frequency response curves of asymmetrical beam in first mode and in presence and absence of the speed fluctuation and different twist angles. As shown in Fig. 9, in absence of the speed fluctuation ($\Gamma 1 = 0$), changes of I_{xx} do not effect on the frequency responses in any twist angle. But, when there is a perturbation on the spinning speed ($\Gamma 1 \neq 0$), ascending the moment of inertia about the x-axis (I_{xx}) increases amplitude and amplifies the speed fluctuation effect (see Fig. 10). However, in this case, it can be seen that ascending the twist angle decreases amplitude of the frequency response and influence of the ascending I_{xx} on the frequency responses. Once again this means that the twist angle can be considered as a damper.

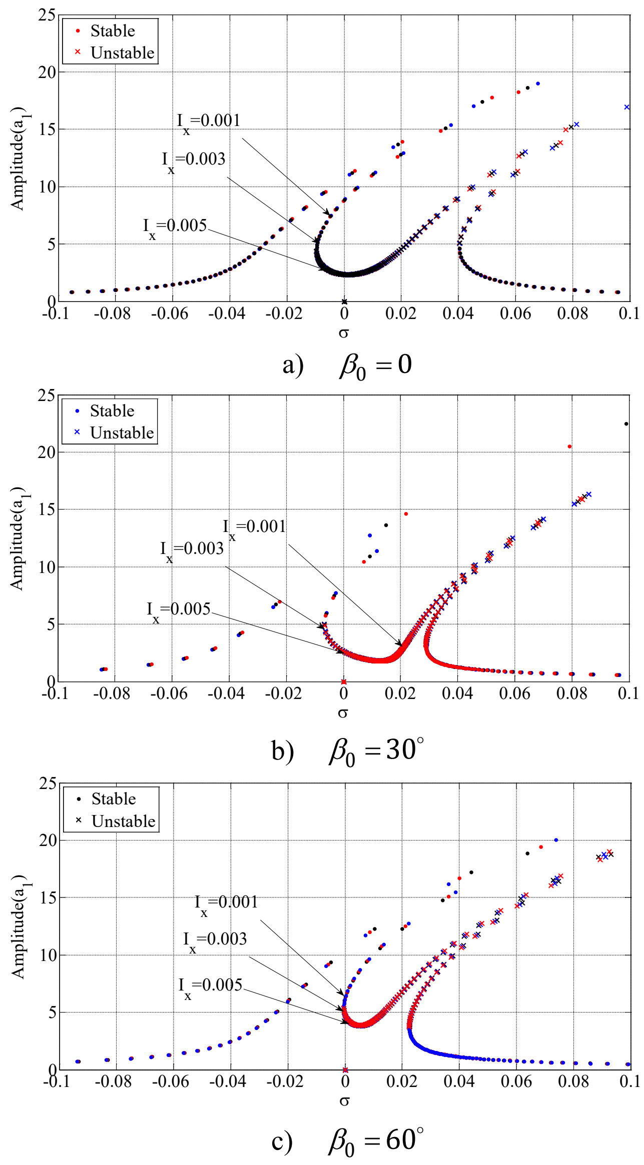

Fig. 10. Influence of the moment of inertia about the x –axis on the frequency response curve of the asymmetrical pre-twisted beam with the speed fluctuation in first mode and different twist angles.

6. CONCLUSION

In this paper, nonlinear instability analysis of the twisted beams with linear twist angle, large transverse deflections and varying spinning speed near the primary and parametric resonances has been. Spinning speed is not constant and the slender twisted beam was modeled with Euler–Bernoulli theory. The equations of motion obtained by Hamilton's principle and were discretized by applying the Galerkin's method. Then multiple scales method was applied on the obtained ordinary differential equations and steady-state analysis of system was done in transverse directions. The accuracy and validation of the obtained results is investigated by comparing the frequency response in first mode and the case $\beta_0 = 0$ with previous researches [45], (Fig. 2). Effects of variations on the amplitude, eccentricity, damping ratio and mass moment of inertia about the x-axis respect to the frequency of the twisted beams are investigated in different pre-twisted angles with and without speed fluctuation, and the stable and unstable zones are determined. Also, the bifurcation diagrams are obtained as a function of control parameters such as frequency, damping ratio and eccentricity in some of the twist angles. Since frequency response curves are bent to the right when spinning speed is constant or variable, the nonlinearity effects are of hardening type and geometrical nonlinearities are dominant in this system. Furthermore, this study explains that the spinning speed fluctuation effect is weak in lower modes and smaller twist angles while asymmetry effect is dominant. By ascending the mode number and twist angle, spinning speed fluctuation effect amplifies the amplitude of system. Hence, it can be said that spinning speed fluctuation effect is considerable in twisted asymmetrical beams by ascending the mode number and twist angles. Also, changing the mass moment of inertia about the x-axis do not change the frequency response curves of the slender beam in absence of the speed fluctuation while in presence of the speed fluctuation, ascending the I_{xx} increases amplitude in any twist angle. However, in any mode, ascending the twist angle decreases ascending effect of the I_{xx} in presence of the speed fluctuation. Finally, Runge-Kutta numerical method is utilized to validate the obtained results analytically and have a good correlation together.

NOMENCLATURE

A	Cross-section of twisted beam, m^2
c_v, c_w	External transverse Damping ratios
c^*	Normalized external damping ratio
$D_{\xi\xi}$, $D_{\zeta\zeta}$, $D_{\eta\eta}$	Torsional and bending stiffness in fixed frame, N/m
E	Young's modulus, Pa
e	Longitudinal strain of centroidal line
e_x, e_y, e_z	Unit vectors of fixed frame
e_η, e_ξ	eccentricity of the cross-section in the twisted frame, m
G	shear modulus, GPa
h_0	cross-section side, m
$I_{xx}, I_{yy}, I_{zz}, I_{yz}$	Moment of inertia and product of inertia in fixed frame, Kg/m^2
$I_{\xi\xi}$, $I_{\zeta\zeta}$, $I_{\eta\eta}$	Moment of inertia in twisted frame, Kg/m^2
J	Jacobian matrix
L	Length of twisted beam, m
m	Beam mass per unit length, Kg/m
n	Mode number
t	Time component, s

t^*	Normalized Time component
u_x, v_y, w_z	displacement components of centroidal line of the twisted beam in fixed frame, m
u_ζ, v_η, w_ξ	displacement components of centroidal line of the twisted beam in twisted frame, m
u_{Gx}, v_{Gy}, w_{Gz}	displacement components of center of mass in fixed frame, m
u^*, v^*, w^*	Normalized displacement components of centroidal line of the twisted beam in twisted frame
X,Y,Z	fixed frame
β_0	pre-twist angle per unit length, rad
ε	very small bookkeeping parameter
Φ_n	Linear mode shape
$\mathcal{L}$	Lagrangian of motion
λ	Eigenvalue of Jacobian matrix
Ω	Spinning speed, rad/s
Ω^*	Normalized spinning speed
ω_f, ω_b	linear forward and backward frequencies, rad/s
$\Re$	transformation matrix of fixed frame to frame
$\Re^T$	Transpose matrix of $\Re$
σ	detuning parameter

Appendix A

Applying the solvability conditions on the Eq. (30) based on the Eq. (31), $G_{f,v}(T_2)$, $G_{b,v}(T_2)$, $G_{f,w}(T_2)$ and $G_{b,w}(T_2)$ are following,

$$\begin{aligned}
G_{f,v} &= \left(\Pi_{1,v} + \omega_f \Pi_{2,v}\right) iA_1' + \Pi_{4,v}\omega_f \\
&\left(\frac{1 - ce^{i\beta_0}}{\beta_0}\right) A_1 + 4\Pi_{3,v}\mu A_1^2 \bar{A}_1 + 8\mu\Pi_{3,v} A_1 \bar{A}_2 A_2 \\
&+1/8\Pi_{5,v}\left(e_\eta + ie_\xi\right)\Omega^2 e^{i\sigma T_2} \\
&+\left[\begin{matrix}\left(-1/2\omega_f\Pi_{1,v} - 1/8\Pi_{3,v}\right) \\ -i\Gamma 1\left(\frac{1-e^{-2i\beta_2}}{\beta_0}\right) + i\Gamma 2\left(\frac{1-e^{-4i\beta_0}}{\beta_0}\right)\end{matrix}\right]\bar{A}_1 e^{2i\sigma T_2}
\end{aligned} \tag{A1}$$

$$\begin{aligned}
G_{f,w} &= \left(-\Pi_{1,v} + \omega_f \Pi_{2,v}\right) A_1' - \Pi_{4,v}\omega_f \\
&\left(\frac{1 - ce^{i\beta_0}}{\beta_0}\right) iA_1 - 4i\Pi_{3,v}\mu A_1^2 \bar{A}_1 - 8i\Pi_{3,v}\mu A_1 \bar{A}_2 A_2 \\
&-1/8\Pi_{5,v}\left(e_\xi - ie_\eta\right)\Omega^2 e^{i\sigma T_2} + \\
&\left[\begin{matrix}\left(-1/2i\omega_f\Pi_{1,v} - 1/8i\Pi_{3,v}\right) + \\ \Gamma 1\left(\frac{1-e^{-2i\beta_2}}{\beta_0}\right) + \Gamma 2\left(\frac{1-e^{-4i\beta_0}}{\beta_0}\right)\end{matrix}\right]\bar{A}_1 e^{2i\sigma T_2}
\end{aligned} \tag{A2}$$

$$\begin{aligned}
G_{b,v} &= 1/2\Pi_{1,w} iA_2' + 1/2\Pi_{2,w}\mu A_2^2 \bar{A}_2 \\
&+\Pi_{2,w}\mu A_1 \bar{A}_1 A_2 + 2n^2\pi^4\left(\frac{1-e^{i\beta_0}}{\beta_0}\right)\omega_b A_2
\end{aligned} \tag{A3}$$

$$\begin{aligned}
G_{b,w} &= 1/2\Pi_{1,w} A_2' - 1/2\Pi_{2,w} i\mu A_2^2 \bar{A}_2 \\
&-\Pi_{2,w} i\mu A_1 \bar{A}_1 A_2 - 2i\pi^2 n^2\left(\frac{1-e^{i\beta_0}}{\beta_0}\right)\omega_b A_2
\end{aligned} \tag{A4}$$

REFERENCES

[1] Washizu, K., Some Consideration on a Naturally Curved and Twisted Slender Beam, Journal of Mathematics and Physics, 43(2) (1964)111-116.

[2] Slyper, H.A., Coupled bending vibrations of pret twisted cantilever beams, Journal of Mechanical Engineering Science, 4(4) (1962)365-379.

[3] Dawson, B., Carnegie, W., Modal curves of pre-twisted beams of rectangular cross-section, Journal of Mechanical Engineering Science, 11(1) (1969)1-13.

[4] Imregun, T., Numerical derivation of FRF matrices for curved, twisted and rotating beams, Journal of Mechanical Engineering Sciences, 203(6) (1989)393-401.

[5] Oh, S.Y., Song, O., Librescu, L., Effects of pretwist and presetting on coupled bending vibrations of rotating thin-walled composite beams, International Journal of Solids and Structures, 40(2003) 1203–1224.

[6] Banerjee, J.R., Development of an exact dynamic stiffness matrix for free vibration analysis of a twisted Timoshenko beam, Journal of Sound and Vibration, 270(1-2) (2004) 379–401.

[7] Yardimoglu, B., Yildirim, T., Finite element model for vibration analysis of pre- twisted Timoshenko beam, Journal of Sound and Vibration, 273(4-5) (2004)741–54.

[8] Subuncu, M., Evran, K., Dynamic stability of a rotating pre-twisted asymmetric cross-section Timoshenko beam subjected to an axial periodic force, International Journal of Mechanical Science, 48(6) (2006)579–90.

[9] Lin, S.M., Lee, J.F., Lee, S.Y., Wang, W.R., Prediction of rotating damped beams with arbitrary pre-twist, International Journal of Mechanical Science, 48(12) (2006)1494–504.

[10] Avramov, K.V., Pierre, C., Flexural-flexural-torsional Nonlinear Vibrations of Pre-twisted Rotating Beams with Asymmetric Cross-sections, Journal of Vibration and Control, 13(4) (2007)329–364.

[11] Verichev, N.N., Verichev, S.N., Erofeyev V.I., Damping lateral vibrations in rotary machinery using motor speed modulation, Journal of Sound and Vibration, 329(1) (2010)13–20.

[12] Yao, M.H., Chen, Y.P., Zhang, W., Nonlinear vibrations of blade with varying rotating speed. Nonlinear Dynamics, 68(4) (2012)487–504.

[13] Ebrahimi, F., Mokhtari, M., Vibration analysis of spinning exponentially functionally graded Timoshenko beams based on differential transform method, Proceedings of the Institution of Mechanical Engineers, Part G: Journal of Aerospace Engineering, 229(14) (2015) 2559-2571.

[14] Bekir, B., Romero, L., Burak, O., Three dimensional dynamics of rotating structures under mixed boundary conditions, Journal of Sound and Vibration, 358(2015)176–191.

[15] Adair, D., Jaeger, M., Vibration analysis of a uniform pre-twisted rotating Euler–Bernoulli beam using the modified Adomian decomposition method, Mathematics and Mechanics of Solids, 23(9) (2017)1345–1363.

[16] Tekinalp, O., Ulsoy, A.G., Modeling and finite element analysis of drill bit vibrations, ASME Journal of Vibration and Acoust, 111(2) (1989)148–55.

[17] Tekinalp, O., Ulsoy, A.G., Effects of geometric and process parameters on drill transverse vibrations, ASME Journal of Manufacturing Science and Engineering, 112(2)) 1990) 189–94.

[18] Huang, B.W., Dynamic characteristics of a drill in the drilling process, Proceeding Instruments Mechanical Engineers Part B, 217(2003).

[19] Young, T.H., Gau, C.Y., Dynamic stability of pre-twisted beams with non-constant spin rates under axial random force International Journal of Solids and Structures, 40(18) (2003) 4675-4698

[20] Gurgeoze, M., On the dynamic stability of a pre-twisted beam subject to a pulsating axial load, Journal of Sound and Vibration, 102(3) (1985) 415-422.

[21] Lee, H.P., Dynamic stability of spinning pre-twisted beams, International Journal of Solids and Structures, 31(18) (1994) 2509–17.

[22] Lee, H.P., Dynamic stability of spinning pre-twisted beams subject to axial pulsating loads, Computer Methods in Applied Mechanics and Engineering, 127(1-4) (1995)115–26.

[23] Tan, T.H., Lee, H.P., Leng, G.S.B., Parametric instability of spinning pre-twisted beams subjected to sinusoidal compressive axial loads, Computers and Structures, 66(6) (1998)745–64.

[24] Chen, W.R., On the vibration and stability of spinning axially loaded pre-twisted Timoshenko beams, Finite Elements in Analysis and Design, 46(11) (2010)1037–47.

[25] Chen, C.H., Huang, Y., Shan, J., The finite element model research of the pre- twisted beam, Applied Mechanics and Materials, 188 (2012)31–6.

[26] Chen, W.R., Hsin, S.W., Chu, T.H., Vibration analysis of twisted Timoshenko beams with internal Kelvin–Voigt damping, Procedia Engineering, 67 (2013)525–32.

[27] Chen, W.R., Effect of local Kelvin-Voigt damping on eigenfrequencies of cantilevered twisted Timoshenko beams, Procedia Engineering, 79 (2014)160-165.

[28] Chen, W.R., Parametric studies on bending vibration of axially-loaded twisted Timoshenko beams with locally distributed Kelvin–Voigt damping, International Journal of Mechanical Sciences, 88 (2014)61-70.

[29] Li, X., Li, Y.H., Qin, Y., Free vibration characteristics of a spinning composite thin-walled beam under hygrothermal environment, International Journal of Mechanical Sciences, 119 (2016)253-265.

[30] Li, X., Qin, Y., Li, Y.H., Zhao, X., The coupled vibration characteristics of a spinning and axially moving composite thin-walled beam, Mechanics of Advanced Materials and Structures, 25(9) (2108) 722-731.

[31] Zhu, K., Chung, J., Dynamic Modelling and analysis of a spinningRayleigh beam under deployment. International Journal of Mechanical Sciences, 115 (2016) 392-405.

[32] Zhu, K., Chung, J., Vibration and stability analysis of a simply-supported Rayleigh beam with spinning and axial motions, Applied Mathematical Modelling, 66 (2019) 362-382.

[33] Thomas, O., Senechal, A., Deu, J.F., Hardening/softening behavior and reduced order modeling of nonlinear vibrations of rotating cantilever beams, Nonlinear Dynamics, 86(2) (2016) 1293-1318.

[34] Sheng, G.G., Wang, X., The geometrically nonlinear dynamic responses of simply supported beams under moving loads, Applied Mathematical Modelling, 48 (2017)183-195.

[35] Farsadi, T., Ozgun, S., Kayran, A., Free vibration analysis of uniform and asymmetric composite pretwisted rotating thin walled beam, (2017)1-22.

[36] Mirtalaie, S. H., Hajabasi, M. A., Nonlinear axial-lateral-torsional free vibrations analysis of Rayleigh rotating shaft, Archive of Applied Mechanics, 87(2017)1465-1494.

[37] Qaderi, M.S., Hosseini, S.A.A., Zamanian, M., Combination parametric resonance of nonlinear unbalanced rotating shafts, 13(11) (2018)1-8.

[38] Xinwei, W., Zhang, X.Y., Three-dimensional vibration analysis of curved and twisted beams with irregular shapes of cross-sections by sub-parametric quadrature element method, Computers and Mathematics with Applications,76(6) (2018)1486-1499.

[39] Karimi Nobandegani, A., Fazelzadeh, S.A., Ghavanloo, E., Non-conservative stability of spinning pre-twisted cantilever beams, Journal of Sound and Vibration, 412 (2018)130-147.

[40] Tajik, M., Karami Mohammadi, A., Nonlinear vibration, stability, and bifurcation analysis of unbalanced spinning pre-twisted beam, Mathematics and Mechanics of Solids, 24(11) (2019)3514-3536.

[41] Nayfeh A.H., Pai P.F., Linear and nonlinear structural mechanics, Edition[1]ed, Wiley Interscience, New York, 2004.

[42] Nayfeh, A.H., Lacarbonara, W., On the discretization of spatially continuous systems with quadratic and cubic nonlinearities, JSME International Journal Series C, 41(3) (1998)510–531.

[43] Nayfeh, A.H., Mook, D.T., Nonlinear oscillations, Edition [1]ed, Wiley Interscience, New York, 1995.

[44] Nayfeh, A.H., Balachandran, B., Applied nonlinear dynamics: analytical, computational, and experimental methods, Edition [1]ed, Wiley, New York, 1995.

[45] Shahgholi, M., Khadem, S.E., Resonance analysis of gyroscopic nonlinear spinning shafts with parametric excitations and speed fluctuations, International Journal of Mechanical Sciences, 64(1) (2012)94–109.

HOW TO CITE THIS ARTICLE

M. Tajik, A. Karami Mohammadi, Effect of Spinning Speed Fluctuation along with the Twist Angle on the Nonlinear Vibration and Stability of an Asymmetrical Twisted Slender Beam, AUT J. Mech Eng., 4(3) (2020) 363-380.

DOI: 10.22060/ajme.2019.16362.5816